

Environmental Applications of Carbon-Based Nanomaterials

MEAGAN S. MAUTER AND MENACHEM ELIMELECH*

Department of Chemical Engineering, Environmental Engineering Program,
Yale University, P.O. Box 208286, New Haven, Connecticut 06520-8286

Received March 8, 2008. Revised manuscript received May 21, 2008. Accepted May 23, 2008.

The unique and tunable properties of carbon-based nanomaterials enable new technologies for identifying and addressing environmental challenges. This review critically assesses the contributions of carbon-based nanomaterials to a broad range of environmental applications: sorbents, high-flux membranes, depth filters, antimicrobial agents, environmental sensors, renewable energy technologies, and pollution prevention strategies. In linking technological advance back to the physical, chemical, and electronic properties of carbonaceous nanomaterials, this article also outlines future opportunities for nanomaterial application in environmental systems.

Introduction

Environmental researchers are actively exploring nanomaterials as contaminants of emerging concern. Articulating the environmental consequences of engineered nanomaterials will inform risk analysis and enable benign nanomaterial design. An exclusive emphasis on implications, however, may overshadow the broad applications of nanotechnology toward improved environmental outcomes. The tunable physical, chemical, and electrical properties of carbon-based nanomaterials inspire innovative solutions to persistent environmental challenges.

Applied nanotechnology research in the biomedical field has charted a path for parallel innovations in environmental science and engineering. Carbonaceous nanomaterials and their functional derivatives are exploited to optimize the fate and transport of drugs through dense tissues (1), specifically target cancerous cells (2), and employ functionalized nanotubes as synthetic transmembrane pores (3). Analogous environmental applications include targeted delivery of remediation agents, engineered removal of hazardous contaminants, and novel membrane structures for water filtration.

The environmental applications of carbonaceous nanomaterials outlined in the review are both proactive (preventing environmental degradation, improving public health, optimizing energy efficiency) and retroactive (remediation, wastewater reuse, pollutant transformation). We begin with a brief outline of carbonaceous nanomaterials and their corresponding properties. We then review leading applications of carbon-based nanotechnologies in the fields of sorption, high-flux membrane separation, depth filtration, pathogen control, environmental sensing, renewable energy production, and pollution prevention.

A suite of new technologies is made possible by recent progress in the rational design and manipulation of nano-

materials. When developed and applied within a sustainable framework, the unique properties of carbonaceous nanomaterials enable environmental applications with limited implications.

Carbon-Based Nanomaterials

Molecular manipulation draws from a broad subset of elements to exploit specific properties on the nanoscale. Structured fullerenes and nanotubes of carbon, boron, MoS₂, WS₂, NbS₂, TiS₂, chrysotile (asbestos), kaolinite, and other precursors demonstrate exceptional physical, mechanical, and electronic properties compared to their bulk forms (4). Carbon's unique hybridization properties, and the sensitivity of carbon's structure to perturbations in synthesis conditions, allow for tailored manipulation to a degree not yet matched by inorganic nanostructures. While inorganic nanomaterials are a promising area of future research, the science and application of carbonaceous nanostructures is more fully developed. The remainder of this paper critically reviews a range of carbonaceous nanomaterials for their application in environmental systems.

The physical, chemical, and electronic properties of carbonaceous nanomaterials are strongly coupled to carbon's structural conformation and, thus, its hybridization state (5). The ground-state orbital configuration of carbon's six electrons is 1s², 2s², 2p². The narrow energy gap between the 2s and 2p electron shells facilitates the promotion of one s orbital electron to the higher energy p orbital that is empty in the ground state. Depending on bonding relationships with the neighboring atoms, this promotion allows carbon to hybridize into a sp, sp², or sp³ configuration. The energy gained from covalent bonding with adjacent atoms compensates for the higher energy state of the electronic configuration. This compensation is nearly equal for the sp² and sp³ hybridization states after the out-of-plane bonding due to π bonds among unhybridized p orbitals is considered (6).

These mutable hybridization states account for the diversity of organic compounds as well as the considerable differences among carbon's bulk configurations (Figure 1). At high temperatures or pressures, carbon assumes the thermodynamically favorable trigonometric sp³ configuration of diamond. At lower heats of formation, however, carbon adopts the planar sp² conformation and forms monolayer sheets bound by three sigma covalent bonds and a single π bond. Weak out-of-plane interactions are a sum of van der Waals forces and the interaction between overlapping π orbitals of parallel sheets. Mild shear forces, physical separa-

* Corresponding author e-mail: menachem.elimelech@yale.edu.

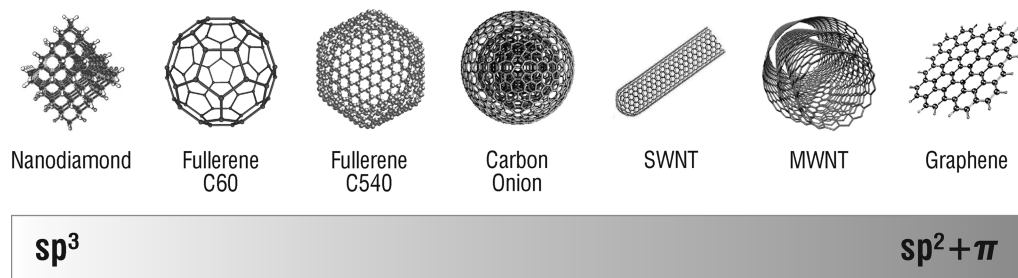


FIGURE 1. Hybridization states of carbon-based nanomaterials. Many chemical and electronic properties of carbonaceous nanomaterials are determined by the dominant hybridization state of the carbon-carbon bonds.

tion, and chemical modification disrupt these weak interplanar forces and cause graphite's planes to slip past each other.

On the nanoscale, graphite sheets are more thermodynamically stable as three-dimensional structures. The strain energy generated by curvature of the planar graphite is compensated by the reduction of unfavorable dangling bonds (7). The result are fullerenes and nanotubes that share many of graphite's attributes, but also exhibit a distinct and tunable set of properties due to quantum effects at the nanoscale, enhanced sp^3 character of the bonds, quantum confinement of wave functions in one or more dimensions (8), and closed topology. Thus, carbonaceous nanomaterials share the same bonding configurations as macroscopic carbon structures, but their properties and morphology are dominated by the stability of select resonance structures rather than the bulk averages of their crystalline forms.

Fullerenes. The electronic structure of fullerenes determines their unique chemical, optical, and structural properties. In defect-free form, fullerenes are enclosed cage-like structures comprised of twelve 5-member rings and an unspecified number of 6-member rings. Structures with fewer hexagons exhibit greater sp^3 bonding character, higher strain energies, and more reactive carbon sites. Isomers with adjacent pentagons also display lower stability and relative abundance than isomers with isolated pentagons in which resonance structures delocalize π bonds over the fullerene structure (9, 10). While the extent of charge delocalization is debated, the chemical behavior of C-60 lies between an aromatic molecule and a straight chained alkene (11).

This balance between stability and reactivity distinguishes Buckminsterfullerene, C-60, from the degenerate C-20 fullerenes and inert, planar graphite. C-60 is an icosahedrally symmetric fullerene (12) stabilized by resonance structures supporting an equivalent electronic state and bonding geometry for each carbon atom (13). The relative stability imparted by this symmetry has redefined C-60 as a starting material for chemical reactions in its own right. Covalent, supramolecular, and endohedral transformations enable molecular manipulation and polymeric material development for specific environmental applications.

Though C-60 is highly resistant to oxidation, up to six electrons can be accommodated in the lowest unoccupied molecular orbital (LUMO). This opens the route to covalent chemistry and the exploitation of fullerenes as structural scaffolding for reactive adducts. Diederich and Thilgen (14) provide an excellent review of the extensive covalent fullerene chemistry that has developed in the past two decades.

Development of supramolecular pathways for fullerene modification has also been critical for exploiting properties relevant to environmental applications. Supramolecular techniques, including molecular self-assembly, are formulated upon noncovalent van der Waals, electrostatic, and hydrophobic interactions intrinsic to fullerenes or their complementary reactants. Of particular relevance to biomedical and

environmental applications are supramolecular techniques to enhance the solubility and reduce the aggregation of hydrophobic fullerene molecules (15). Such techniques have refined control over secondary architectures ranging from monolayered films to complex three-dimensional macrostructures (16). Combinations of covalent and supramolecular techniques have further expanded the range of tailored structures available (17).

The electric and conductive properties of fullerenes and other carbonaceous nanomaterials form the basis for many of their unique characteristics on the nanoscale. Thus, modification of these electric properties via single substitution or endohedral doping has generated significant research attention. Single atom substitutions in a fullerene structure have ramifications for the photosensitivity and binding energies of the fullerene molecule (18). With an internal diameter of 0.7 nm (19), the C-60 fullerene cage may also be endohedrally doped for electronic modification, transport of interstitial atoms, or dissolution and vaporization processes of otherwise refractory metals (20). Select endohedral dopants induce rehybridization of the fullerene molecule via ionic interactions and charge transfer (21), whereas others exhibit little effect on the basic properties of the fullerene molecule.

Carbonaceous nanomaterial research has also characterized other fullerene conformations including a group of very large spherical fullerenes (22, 23) and a class of concentric fullerenes titled carbon onions (24). The exceptional reactivity of these molecules is a function of symmetry and bonding conformation. Theory predicts that large fullerenes and carbon onions adopt a faceted structure. Direct imaging, however, indicates that these molecules maintain the spherical geometry of C-60. This discrepancy between theory and observation has prompted the suggestion that Stone-Wales defects are an integral part of the standard bonding structure (25). Stone-Wales defects describe the rearrangement of four six-member rings into a 5-7-7-5 conformation (26). The diminished resonance and higher strain energy of this conformation increases the probability of nucleophilic attack, providing one possible explanation for enhanced reactivity.

An important physicochemical attribute of fullerenes is their tendency to form stable crystalline nanoparticles (25–500 nm in diameter) in a variety of solutions, including water at environmentally relevant pH and electrolyte concentrations (27–30). In the absence of humic acid, aggregation behavior of the fullerenes is consistent with the classic Derjaguin-Landau-Verwey-Overbeek (DLVO) theory of colloidal stability (28). Average aggregate diameter exhibits dependence on pH, ionic strength, mixing behavior, initial fullerene concentration, and time in solution (31–33). In the presence of humic acid, however, adsorption of macromolecules to the fullerene nanoparticles induces steric stabilization and sharply reduces aggregation rates (34).

Nanotubes. Carbon nanotubes (CNTs) (35) are the one-dimensional analogues of zero-dimensional fullerene

		Environmental Applications						
		Pollution Prevention	Sorbents	Composite Filters	Energy Storage	Antimicrobial Agents	Aligned CNT Membranes	Sensors
Physical Properties	Size		X	X		X	X	X
	Shape					X	X	
	Surface Area	X	X	X	X			
	Molecular Specificity		X		X			X
	Hydrophobicity		X	X		X	X	
	Electrical Conductivity				X			X
	Optical Activity		X					
	Thermal Conductivity	X			X			
Bulk Properties		X						
Individual Properties			X					

FIGURE 2. Application of carbonaceous nanomaterials' unique properties in environmental systems. Both individual and bulk configurations of carbonaceous nanomaterials display unique properties. Further characterization of carbon-based nanomaterial attributes, synthesis techniques, and purification procedures will expand their range of environmental applications.

molecules. Conceptually, a nanotube is a micrometer-scale graphene sheet rolled into a cylinder of nanoscale diameter and capped with a spherical fullerene. Paring a nanoscale diameter with a micro- to centimeter length produces CNT structures of exceptional aspect ratio. Extensive reviews have been published on the synthesis and structural conformation of CNTs (6, 36–38). This brief introduction to CNTs highlights their position on the spectrum of carbon hybridization and the effect that this conformation has on properties relevant to environmental applications.

As with spherical fullerenes, the sidewalls of CNTs share graphene's hexagonal sp^2 conformation. Unlike their zero dimensional counterparts, however, the degree of curvature in nanotubes is confined to a single dimension. The stronger sp^3 character of this bonding conformation reduces the strain energy on the sidewall carbons and renders CNT less susceptible to chemical modification and rearrangement than spherical fullerene molecules.

Nanotubes, however, are distinct from graphene planes on two important accounts. First, the one-dimensional geometry of the tubule induces quantum confinement in the radial and circumferential directions (8). Second, the potential for structural indeterminacy is introduced when graphene's two-dimensional hexagonal carbon conformation is confined to a single dimension. Indeed, the orientation of the rolled graphene sheet has a profound impact on the electronic properties of the CNT. While bulk graphite is a semiconductor, isolated single-walled nanotubes (SWNTs) of small diameter exhibit metallic, semimetallic, or semiconducting behavior depending on this orientation of the hexagonal lattice (39). In high yield synthesis techniques, the majority of the nanotubes adopt a metallic armchair conformation (5), though difficulties in purifying for monochiral nanotubes constrain commercial and environmental applications of SWNTs.

Double-walled and multiwalled nanotubes (MWNTs) are the one-dimensional analogues of carbon onions. As with concentric fullerenes, MWNTs share many of the same characteristics of bulk SWNTs since coupling across the 0.34 nm interlayer distance (40) of MWNTs is weak. MWNTs do not exhibit the metallic properties of SWNTs, instead displaying the semiconducting characteristics of bulk graphite.

Strong attractive forces between nanotubes complicate CNT purification and manipulation. These forces account for CNTs' tightly bundled conformation (41) and low disper-

sion in both polar and apolar solvents. Often a physical dispersion process, such as sonication, is necessary to debundle nanotube sheaths. Other techniques include exfoliation with natural polyelectrolytes (42), aromatic polymers (43), or DNA (44). In these supramolecular debundling routes, the aromatic constituents of the exfoliating agent interact with the π orbitals of the nanotube sidewall to sterically interfere with bundling (42). While supramolecular techniques are effective in dispersing the CNT bundles, their applicability is limited in systems utilizing the properties of pristine nanotubes.

This difficulty in dispersion complicates the covalent and supramolecular modification techniques that have been developed for more highly soluble fullerenes. While extensive functionalization and supramolecular modifications have been developed (45–49), the range and control of molecular manipulation is more difficult for nanotubes. The reduced strain energy of the sidewall hexagons further diminishes the reactivity of the carbons and necessitates stronger reagents. The functionalization chemistry of SWNTs is similar to that described for fullerenes, with details provided in several reviews (50, 51).

Finally, commercially available SWNTs and MWNTs are replete with defects, metal catalyst contamination, and physical heterogeneities. While a number of purification schemes have been developed (52–54), variation between samples is a challenge for research on the implications and commercial applications of CNTs (55). Due to these inconsistencies in synthesis, the majority of proposed environmental applications of CNTs draw upon bulk properties, such as high surface area, rather than single nanotube properties such as high conductivity or efficient field emission.

Unique Properties of Carbon-Based Nanomaterials

Carbonaceous nanomaterials unite the distinctive properties of sp^2 hybridized carbon bonds with the unusual characteristics of physics and chemistry at the nanoscale. From the electrical conductivity of a single nanotube to the adsorptive capacity of bulk nanomaterials, both single molecule and bulk properties offer potential advances in environmental systems (Figure 2). The unique properties of carbonaceous nanomaterials most commonly cited in environmental applications are size, shape, and surface area; molecular

interactions and sorption properties; and electronic, optical, and thermal properties.

Size, Shape, and Surface Area. Molecular manipulation implies control over the structure and conformation of a material. For carbonaceous nanomaterials this includes size, length, chirality, and the number of layers in the fullerene cage. Although current fabrication techniques for nanoscale carbon structures lack complete precision and uniformity, links between growth conditions and product properties inform the synthesis of tuned nanomaterials. Variations in synthesis technique, temperature, pressure, catalyst, electron field, and process gases optimize nanomaterial structure, purity, and physical orientation for specific applications (38, 56–58). For instance, SWNT diameter is strongly correlated to synthesis technique, with HiPCO synthesis capable of yielding nanotubes between 0.7 and 1 nm. Laser ablation and other graphitic based techniques produce slightly larger nanotubes in the range of 1–2 nm (47).

Diameter is a critical dimension in determining the properties and applications of fullerene and tubular nanostructures. In fullerenes, diameter is referenced by the number of carbons in the spherical molecule. For C-60, the smallest fullerene obeying the stabilizing pentagon isolation rule, the inner diameter approaches 0.7 nm. This is also the lower range for SWNT diameters, though average diameters of 1.4 nm are reported across a number of commercial synthesis techniques (59). Small SWNT diameters induce higher strain energies, mixing of the σ and π bonds, and electron orbital rehybridization. These bond structure modifications induce fundamental alterations to the electronic, optical, mechanical, elastic, and thermal properties of SWNTs.

The characteristic properties dependent on nanotube diameter are complemented by physical size exclusion and capillary behavior relevant to environmental systems. The narrow inner diameter of nanotubes has found application in novel molding, separation, and size exclusion processes including nanowire synthesis (60) and membrane filtration (61). These constrained inner diameters, however, have also hindered CNT applications by complicating purification methods for eliminating growth catalysts from bulk nanotubes (54, 62). The combined characteristics of narrow diameters and long tubules also imply exceptional aspect ratios in nanotubular structures. Further details on the properties and applications of high aspect ratio nanomaterials are collected in the referenced reviews (37, 63–65).

Across the spectrum of carbonaceous nanomaterials, the high surface area to volume ratio distinguishes nanomaterials from their micro- or macro-scale counterparts. As clusters of atoms approach the nanoscale, the ratio of $\Delta G_{\text{surface}}/\Delta G_{\text{volume}}$ increases, where ΔG represents the difference in free energy between the bulk material and the nanoscale structure (66). The higher percentages of surface atoms confer adsorptive capacity and broad application as a scaffolding material for species localized to the nanotube surface (67–70).

Finally, while most literature addresses the physical properties of individual nanomaterials, the size, shape, and surface area of carbonaceous nanomaterials are highly dependent upon aggregation (bundling) state and solvent chemistry. Impurities—including vapor, biomolecules, and metals—that adsorb to the surface of nanomaterials may fundamentally alter the aggregation behavior, thermal and electric characteristics, mechanical strength, and physicochemical properties of the nanomaterials. The physicochemical properties attributed to secondary structures of nanomaterial aggregates are highly variable and poorly characterized. Resolving these characteristics is imperative for widespread application of carbonaceous nanomaterials from both technical and environmental health and safety perspectives.

Molecular Interactions and Sorption Properties. Elucidating the molecular interactions, sorption, and partitioning properties governing fullerenes and nanotubes is a joint effort between theorists and experimentalists. Carbonaceous nanomaterials are generally consistent with traditional physical–chemical models and theories including electrostatics (71), adsorption (72), hydrophobicity (73), and Hansen solubility parameters (74). Molecular modeling has provided a rendition of physical–chemical processes at the nanoscale that are otherwise inaccessible through experimental techniques (75), though computational demands limit the range of length-scale, chirality, and layers feasible in the molecular modeling of heterogenous nanotube samples.

The potential energies of interaction between carbonaceous nanomaterials are described by the classic Lennard-Jones (LJ) continuum model (76, 77). The LJ model accounts for both van der Waals attractive forces (Kessom, Debye, and London forces) and Pauli repulsion originating from overlapping electron orbitals at very short separation distances (66). Geometry-specific empirical constants provide strong correlation to the theory of a universal graphitic potential when geometries are considered (76).

Electrostatic interactions between fullerene nanoparticles are also consistent with the classic DLVO theory of colloidal stability, although the origin of fullerene nanoparticle surface charge in aqueous solutions is not fully understood (28). Functionalization via covalent or supramolecular techniques reduces aggregation through steric hindrance and the introduction of polar functional groups that confer hydrophilicity to the otherwise hydrophobic nanoparticles (11, 14, 17, 34, 78). Aggregation kinetics measurements of fullerene nanoparticles in aqueous solutions of 1:1 electrolytes yield an effective Hamaker constant of 6.7×10^{-21} J, consistent with organic and biological particles in aqueous media (28).

Hydrophobicity relates the strength of water–water interactions to water–particle and particle–particle interactions. A hydrophobic molecule will interact less favorably with water than two solute molecules interact with each other, causing the liquid to withdraw from the surface and form a vapor layer (79). The hydrophobic characteristics of C-60 and CNTs induce drying and the expulsion of interstitial water over short length scales and strongly influence their aggregation state (73). Molecular simulations of CNT in water suggest that the primary barrier to dissolution is the energy required to disrupt water–water bonds when forming a cavity for the CNT (80).

Early work suggested capillary forces in nanotubes would be incredibly strong, drawing molecules from vapor or liquid phases into the molecular “straws” by way of van der Waals attractive forces and dipole–induced dipole interactions with polar molecules (81). This work was incomplete, however, in that it omitted wetting as a factor in the nanotube capillarity. Dujardin et al. (82) revised this model, incorporating the Laplace equation into predictions of nanotube capillarity for a variety of metals.

The entropic costs of water confinement and the enthalpic loss from reduced hydrogen bonding partners are compensated by enhanced electrostatic interactions due to the diminished polarizability of the medium (75). Liquids with high surface tension do not wet nanotubes, whereas water and most organic solvents either have low enough cohesive forces or strong enough intermolecular interactions with the nanotube surface to induce capillary action (83). Surface tension limits for wettability are estimated to be in the range of 72 mN/m (82, 83). The Laplace equation predicts an inverse relationship between the pressure differential driving capillary action and the radius of curvature of the nanotube. Thus,

the internal diameter of the nanotube may significantly alter the properties of fluid flow and capillarity.

Hydrophobicity and capillarity also contribute to the adsorption behavior and orientation of sorbates in microporous carbons. Physisorption is the dominant mechanism of sorption for unfunctionalized nanomaterials (84). Adsorption studies report rapid equilibrium rates, high adsorption capacity, low sensitivity to pH range, minimal hysteresis in dispersed nanoparticle samples (85), and consistency with traditional Langmuir, BET, or Freundlich isotherms (72, 84, 86).

Nevertheless, these studies are complicated by unique properties of adsorption in micropores. In particular, the increase in dispersion energy and the overlapping force fields from adjacent carbon walls magnify sorbent–sorbate and sorbent–sorbent interactions causing condensation inside of the nanotube (84). This so-called filling of nanotubes may explain why some models describe adsorption capacity above the physical surface area of a CNT (72, 87–89). In environmental applications, adsorptive capacity has broad implications for contaminant removal and hydrogen storage.

Electronic, Optical, and Thermal Properties. The bonding configuration of fullerenes and nanotubes confers unique conductive, optical, and thermal properties offering broad promise for application in the electronic industry. While the relevance of unique field emission properties, optical non-linearity, high thermal conductivity, and low temperature quantum phenomena may seem distantly related to traditional environmental applications, substantial indirect environmental benefits accrue from redesign of energy and material intensive consumer electronics (90). Novel electronic properties of carbon-based nanomaterials will also contribute to environmental sensing devices and efficient power generation in innovative solar cell architectures (91). Finally, fullerene mediated photooxidation of persistent organics has been explored as an environmental remediation technique (92–95).

Fullerenes are notable for optical activity over both the UV and visible ranges. The strong absorption bands are attributed to electron transitions from bonding to antibonding orbitals in the UV range and between the HOMO and LUMO bands in the visible range. Strong UV absorption also induces photoexcitation of the fullerene molecule from a ground level state to a singlet excited state. Although this excited-state decays within approximately 1.2 ns (96), the emission wavelength is capable of generating a range of reactive oxygen species (ROS), including singlet oxygen molecules, superoxide radical anions, and hydroxide radicals in aqueous media containing common environmental solutes (97). Hotze et al. (98) provide a mechanistic framework for photosensitization that accounts for differences in the aqueous phase aggregate structure between fullerol and nC-60. Water-soluble fullerol displays high quantum yields and efficiently generates ROS (99). In crystalline nC-60 nanoparticles, however, the dense packing of the fullerene molecules induces triplet–triplet annihilation and self-quenching to sharply reduce the photochemical reactivity of (97, 98). ROS generation has raised concerns about the biocompatibility of fullerenes in aqueous media and the importance of understanding the aggregation state of nanomaterials in the environment (27, 100).

Tunable band gaps, remarkably stable and high current-carrying capacity, low ionization potential, and efficient field emission properties (101) are the most highly cited electronic properties of SWNTs. Many of these properties stem from electron flow confinement in one-dimensional nanotubes (5). The electronic properties of nanotubes are closely linked to chirality, diameter, length, and the number of concentric tubules (102). In general, the heterogeneities of MWNTs

induce defect scattering and diffusive electron motion (103–105), which reduce their applicability in environmental and consumer products.

Theoretical and experimental work demonstrates that band gaps are dependent upon the chirality and diameter of nanotubes. A reference coordinate system indexes the chirality of the SWNT by a pair of (n , m) integers corresponding to specific atoms on a planar graphene sheet (38). Armchair conformations, denoted by (n , n) tubes, are metallic (i.e., zero band gap) and independent of tube diameter and curvature. The (n , m) nanotubes, with carbon atoms arranged in a zigzag or helical conformation, are small gap or large gap semiconductors. As the radius of these semiconducting nanotubes increases, the gaps decay as $1/R$ or $1/R^2$, with R being the nanotube radius, until the tubes display metallic properties similar to the armchair configuration (38). Conduction in MWNTs is dominated by the electronic structure of the outermost tubules and resembles the electronic behavior of graphite (5).

Metallic SWNTs behave as quantum wires, with electron confinement in the radial direction quantizing the conduction bands into discrete energy levels (104, 106). Electrons are transported via resonant tunneling through these discrete electron states in the nanotube, and are delocalized over some extended length of the nanotube. This spatial extension of charge not only enhances conductivity and current capacity, but it also reduces the influence of defects in the nanotube sidewalls. Select dopants also increase conductivity, either by serving as intercalates to facilitate charge transfer between the planar structure of the sp^2 hybridized sidewalls (107, 108), or by altering the local electronic density of states to create metallic features (109). Conductivity in quantum wires is very sensitive to adsorption by surrounding liquid or gaseous molecules, and, in this role, SWNTs have found broad applications as environmental sensors (110–113).

The ionization potential of SWNTs is below that of many common field emitters currently used in the electronics industry. Ionization potential refers to the energy necessary to excite an electron from the ground-state to an excited state. In field emitters, a low ionization potential reduces the voltage necessary for exciting an electron and forcing its emission from the molecule. Other SWNT properties useful in field emission include charge delocalization to prevent a build up of electron holes on the nanotube and narrow diameters to spatially direct electron emission (101). Further reduction in ionization potential is observed in the presence of certain adsorbates, including water (114). Reducing the voltage potential and enhancing the efficiency of field emission is one example of nanotube application in the green design of next generation devices.

Finally, both individual tubules and bulk assemblies of CNTs exhibit high thermal conductivity (115–117). The primary barrier to thermal conductivity on the bulk scale occurs at tube–tube junctions. Recent progress in joining nanotubes (65) may facilitate the development of long fibers with high thermal conductivity.

Carbonaceous Nanomaterials as Sorbents

Sorption of environmental contaminants to sorbents such as NOM, clay, and activated carbon accounts for a major sink in natural and engineered environmental systems. Conventional drinking water treatment, for example, relies on physicochemical sorption processes for the removal of organic and inorganic contaminants. Decades of research have enhanced our understanding of sorption mechanisms and facilitated optimization of sorbent properties (118–123).

The sorptive capacity of conventional carbonaceous sorbents is limited by the density of surface active sites, the

activation energy of sorptive bonds, the slow kinetics and nonequilibrium of sorption in heterogeneous systems, and the mass transfer rate to the sorbent surface. The large dimensions of traditional sorbents also limit their transport through low porosity environments and complicate efforts in subsurface remediation. Carbonaceous nanosorbents, with their high surface area to volume ratio, controlled pore size distribution, and manipulatable surface chemistry, overcome many of these intrinsic limitations. Sorption studies using carbon-based nanomaterials report rapid equilibrium rates, high adsorption capacity, effectiveness over a broad pH range, and consistency with BET, Langmuir, or Freundlich isotherms (124–129).

Direct sorption of organic contaminants to the nanomaterial surface is driven by the same fundamental hydrophobic, dispersion, and weak dipolar forces that determine sorption energies in conventional systems (118, 119). The higher equilibrium rates of carbonaceous nanosorbents over activated carbon are attributed to π electron polarizability or π - π electron-donor-acceptor (EDA) interactions with aromatic sorbates (86, 130, 131), reduced heterogeneity of adsorption energies (132), and the absence of pore diffusion as an intermediate mechanism in adsorption (133). This conclusion is reinforced by the work of Yang et al. (134) comparing a variety of carbonaceous nanosorbents including C-60, nC-60 nanoparticles, SWNTs, and varying dimensions of MWNTs. Another advantage to carbonaceous nanosorbents is the virtual absence of hysteresis between adsorption and desorption isotherms for liquids and gases under atmospheric pressure (85, 135). Enhanced atmospheric pressure, relevant to gas adsorption in hydrogen storage applications, may restore hysteresis in the system by reducing the energy barrier to fill nonwetting CNT pores and the intraparticle region of nC-60 aggregates (135–137).

The nonspecific van der Waals interactions driving adsorption to SWNTs are amplified by enhanced interaction potentials in systems with curved geometries. Monte Carlo simulations have been used to predict an optimal pore diameter for gaseous adsorption to SWNTs. For the adsorption of tetrafluoromethane, a potent greenhouse gas, 1.05 nm is the optimal nanotube diameter for balancing the strong binding energies (enthalpy of adsorption) against the total volume available for gas storage (138). Similar models may be used to predict optimal carbon nanostructures for the removal of target contaminants.

Traditional applications of activated carbon in water and wastewater treatment include reduction in organic contaminants, residual taste, or odor. While carbonaceous nanosorbents are effective in these areas, their cost and possible toxicity have prevented extensive research in direct and widespread use for water treatment. Savage and Diallo (139) have proposed integration of nanosorbents into traditional packed-bed reactors, though details on the effectiveness of various nanomaterial immobilization strategies have not been presented. To date, most research on the environmental applications of nanosorbents has targeted the removal of specific hazardous contaminants such as trihalomethanes (124), polycyclic aromatic hydrocarbons (134), or naphthalene (128).

While rapid equilibrium rates and high sorbent capacity are powerful attributes of carbonaceous nanosorbents, they are essentially incremental advances upon an existing paradigm. The true revolutionary potential of nanosorbents lies in the diverse pathways for tailored manipulation of fullerene and nanotube surface chemistry. Tailoring the dominant physical and chemical adsorption forces via bottom-up synthesis and selective functionalization yields carbonaceous nanomaterials that complement the existing suite of relatively unspecific conventional sorbents. Functionalized nanosor-

bents may provide an optimized approach for targeting specific micropollutants, removing low concentration contaminants (140), or improving subsurface mobility (141). For instance, when compared to activated carbon, CNTs functionalized with hydrophilic $-\text{OH}$ and $-\text{COOH}$ groups exhibited superior sorption of low molecular weight and polar compounds (124).

In contrast to the relatively nonspecific, hydrophobic sorption mechanisms describing organic sorption, inorganic sorption to carbonaceous nanostructures is characterized by specific complexation reactions. Surface functional group density, rather than total surface area, becomes the primary determinant of inorganic sorption capacity. Metal speciation or competing complexation reactions also render sorption capacity sensitive to changes in pH (142–144). Finally, sorption of oxyanion metal contaminants, such as arsenic, varies with the concentration of divalent cations in solution, possibly due to cationic bridging of the metal to deprotonated oxygen groups on the sorbent surface through a ternary surface complex reaction (145).

In addition to serving as direct sorbents, carbonaceous nanomaterials have also been employed as a high surface area scaffold for oxides or macromolecules with intrinsic sorbent capacity. Covalent chemistry opens synthesis routes for nanoscaffolds tailored to adsorb or complex ions, metals, and radionuclides in solution. Recent examples of nanomaterials as scaffolding agents for contaminant removal include CNT decoration with ceria (CeO_2) nanoparticles for arsenate and chromium removal (145, 146), amorphous alumina for fluoride adsorption (147), and polypyrrole for perchlorate separation (67). Current applications have focused on metal preconcentration, removal, or oxidation.

Despite high synthesis costs, the cost effectiveness of single-walled and multiwalled nanosorbents over traditional activated carbon was recently demonstrated (148). Of course, cost-effective environmental applications of nanomaterials' sorptive capacity are not limited to the removal or remediation of common contaminants. Fullerene and MWNT-assisted preconcentration of metals (149, 150), adsorption of hydrogen to SWNTs in fuel cells (151), viral adsorption to SWNT-based drinking water filters, and the use of CNTs as single molecule environmental sensors (152) are addressed in subsequent sections of this review.

Aligned CNTs as High-Flux Membranes with Tailored Selectivity

Traditional reverse osmosis (RO) desalination membranes separate components based upon their solution-diffusion rates through a dense polymeric film barrier. This separation mechanism forces a fundamental tradeoff between high selectivity and water flux in current membrane design. While polymeric RO membranes are likely to remain the dominant desalination technology, further improvements to diffusion based membrane performance are expected to be incremental. Novel membranes drawing on the unique properties of CNTs may reduce significantly the energy and cost of desalination (153).

Nanotube-based filtration membranes (Figure 3), in which aligned nanotubes serve as pores in an impermeable support matrix, were first introduced by Jirage et al. (154). In separation experiments with a mixture of two organic solutes, the tailored shape and uniform inner diameter of the gold nanotubes selected for low molecular weight solutes while maintaining high permeate flux. Further development of sterically selective membranes has drawn upon the tunable properties and broad functionalization pathways of CNTs to augment steric selection with chemical- and/or charge-based selectivity. Membrane optimization includes adjustments to

Gold nanotubule
(Jirage et al., 1997)

Macromolecular separation.

Bottle-neck tubule
(Jirage et al., 1997)

Narrow entrance, wide pore for increased flux.

Aligned MWNT membrane
(Hinds et al., 2004)

Oxidized nanotube tips for high-flux separation.

Functionalized MWNT membrane
(Majumder et al., 2005)

Macromolecular functionalization for tunable nanofiltration.

Aligned DWNT
(Holt, 2006)

Narrowed diameter for nanofiltration and potential brackish H₂O desalination.

Polarized and voltage-dependent wetting
(Wang et al., 2007)

Controllably wicks fluids for nanofluidics applications.

Next generation membranes:

Aligned SWNT

Desalination.

Functionalized SWNT

Functionalization for tailored selectivity and fouling resistance.

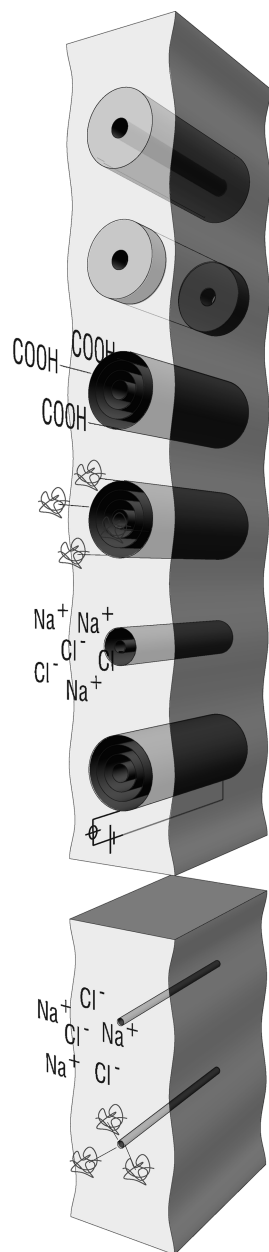


FIGURE 3. Evolution of aligned nanotube membranes for chemical separation and water treatment applications. Carbon nanotube membranes have evolved from size exclusion sieving devices to tunable membranes for nanofiltration. Future research is focused around the development of a high-flux, antifouling SWNT membrane for desalination applications.

pore diameter (61), surface hydrophobicity (155), and nanotube tip functionalization for channel gating (156, 157). The inherent symmetry of these aligned nanotube membranes also eliminates the internal concentration polarization effect that has hindered the implementation of traditional asymmetric membranes in emerging desalination and other osmotically driven membrane-based technologies such as forward osmosis and pressure retarded osmosis (158–160).

Recent experimental investigations show promise for advanced water treatment applications of high-flux aligned CNT membranes. Hinds et al. (161) aligned MWNTs within a polymer film to form a nanoporous membrane structure. The broad inner diameter (>4 nm) and distribution of pore sizes reported for this early membrane, however, are better suited to ultrafiltration than desalination. Holt et al. (61) improved upon size selectivity while maintaining high mass

transport rates in a membrane of aligned double-walled CNTs with an inner diameter less than 2 nm.

Aligned CNT membranes display flow rates 4–5 orders of magnitude higher than predicted by conventional fluid-flow theories (162). Theoretical studies to understand the origin of these high flow rates suggest that together the nanoscale channels, hydrophobicity (82), and smooth internal walls (163) of CNTs act to reduce the frictional forces upon passing water molecules (164). Confinement of water molecules within narrow diameter CNTs induces molecular alignment (165) and phase transitions (166) uncharacteristic of bulk water. This alignment enhances hydrogen bonding among water molecules and introduces a vapor phase barrier separating the chain of water molecules from the nonpolar surface of the carbon sidewall (79).

Past research has demonstrated that nonwetting solid–fluid interfaces may violate the no-slip boundary condition imposed by the Hagen–Poiseuille equation (167, 168). Long slip lengths diminish wall effects, permitting rapid flow through confined pores. Limited boundary effects also reduce flow dependence on physical properties such as fluid viscosity (162) and the length of the nanotube pore (169). The exceptionally long slip lengths calculated for CNTs are directly related to their hydrophobicity and atomic smoothness (162, 170, 171). Molecular dynamics simulations provide detailed information on flow properties through individual CNTs (79, 165, 172) and aligned CNT membranes (169, 173, 174).

Flow rates are governed by end processes and physical barriers at the nanotube channel’s inlet and outlet (161). Oxidation or chemical modification of the CNT tips with hydrophilic functional groups increases the binding energy between water and the nanotube to enhance membrane flux (175). While tip functionalization inevitably proceeds from opening the nanotube ends during membrane synthesis, the resulting carboxylic acid groups can be further derivitized under a range of chemical reactions (156).

Functional group channel gating of large nanotube pores has refined the selective capacity of CNT membranes. Majumder et al. (156) separated two differently sized, but identically charged, particles by modifying the length and structure of the functional groups at the nanotube tips. This separation mechanism reduces membrane selectivity’s dependence on small variations in the nanotube diameters, but steric separation techniques may also reduce membrane permeability and flux. For example, functionalization with bulky streptavidin molecules was shown to completely and reversibly eliminate transport through the membrane (157). High-flux nanotube membrane design must balance these competing forces of selectivity and permeability.

While the aforementioned membranes are highly relevant to nanofiltration, no studies on aligned nanotube membranes have demonstrated salt rejection at concentrations relevant for desalination (176). Although negatively charged functional groups at the CNT tips result in salt rejection by charge (Donnan) exclusion (176, 177), the efficiency of this mechanism declines significantly as the ionic strength or divalent cation concentration increases. The high ionic strength of seawater thus eliminates charge exclusion as a practical separation mechanism for channel gated CNT membranes.

The hydrated radius of sodium ions ranges from between 0.178 and 0.358 nm, depending upon environmental conditions including ionic strength, pH, and temperature (178, 179). To achieve desalination, the pore size distribution must be narrowed via fabrication of a SWNT membrane with subnanometer pores or steric channel gating. Subsequent iterations in CNT membrane design must also consider membrane fouling behavior, scaling to membrane modules, and membrane fabrication costs.

Aligned CNT membranes may find additional application in nano- and microfluidic systems, where the precise handling of small samples is critical for analytical separation or laboratory-on-chip devices. When a voltage is applied across the aligned CNT membrane, the nanotube tips transition from uncharged and superhydrophobic to charged and hydrophilic (180). This modification of physicochemical interactions between the fluid and the nanotube enables the controlled wicking of fluids and tight regulation of both flow rate and direction (155, 175, 181). Alternatively, Li et al. (182) draw upon the correlation between pore compression and solvent flux in compression-modulated tunable-pore carbon-nanotube membrane filters for molecular separation. In this scheme, the selectivity and permeability of the CNT membrane are dynamically tuned under different degrees of uniaxial compression.

Carbonaceous Nanomaterials for Composite Filters

While aligned CNT composite membranes produce highly specific, tunable, and rapid filtration on the bench scale, they are difficult to manufacture and are still in the early stages of research and development. Alternative CNT applications in nanocomposite membranes utilize the physical properties of CNTs to improve upon the mechanical stability of the membrane or as a tool to disrupt polymer packing of the active layer in traditional reverse osmosis membranes (183–185).

Wang et al. (186) report on high-flux filtration membranes with a hydrophilic nanocomposite surface coating. These membranes consist of a dense hydrophilic nanocomposite coating top layer, an electrospun polyvinyl alcohol (PVA) substrate midlayer, and a conventional nonwoven microfibrillar support layer. The incorporation of MWNTs into the hydrophilic top layer improved mechanical strength and durability while simultaneously enhancing water permeability. Increasing concentration and oxidization of the MWNTs also enhanced water permeability, suggesting that the MWNTs improve flow by disrupting polymer chain packing and creating nanoscale cavities in the coating layer. Wang et al. (186) also hypothesize that direct flow through the center of the frictionless MWNTs contributed to the high water flux through the membrane, although the same problems of pore blockage and low vertical alignment that plague aligned CNT membranes make it unlikely that intratubular transport contributes significantly to enhanced flow.

Choi et al. (185) optimized the performance of an asymmetric MWNT/polymer blend ultrafiltration membrane by altering the concentration of oxidized MWNTs. A 1.5 wt % of MWNTs maximized the porosity of the composite membrane by increasing viscosity and reducing thermodynamic stability of the casting solution. Higher loadings of oxidized MWNTs, up to 4 wt %, in the casting solution simultaneously improved flux and solute rejection. While this research highlights opportunities for careful tuning of membrane properties based upon the physicochemical characteristics and concentration of MWNTs, the absence of mechanistic explanations for changes to flux and solute rejection hinder rational membrane design.

Subsequent composite membrane designs combine enhanced flow rates with other unique properties of carbonaceous nanomaterials, including sorptive capacity, antimicrobial activity, and thermal stability. Poly(2,6-dimethyl-1,4-phenylene oxide) (PPO)-fullerene composite membranes for the treatment of dissolved estrogenic compounds enhance permeate flux through controlled heterogeneity in the polymer chain packing while simultaneously improving the adsorption rate and capacity of the membrane for

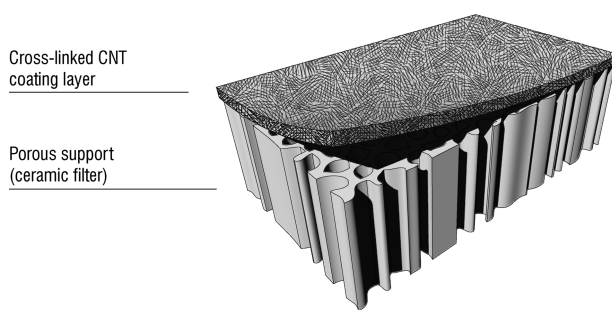


FIGURE 4. Schematic of CNT hybrid filter. A cross-linked CNT filtration layer atop a porous ceramic support provides the basis for a robust, regenerative water purification device.

hydrophobic organics (187). Assuming immobilization of the nanomaterials can be demonstrated over the membrane lifespan, this may be a low risk and efficient way to apply the unique properties of nanomaterials toward water and wastewater treatment.

The narrow diameter, high surface area, thermal resistance, and porous aggregate structure of SWNTs are also applicable in regenerative hybrid ceramic filters. Building upon earlier demonstrations of MWNT filter efficacy in bacterial removal (188), recent work describes a highly permeable SWNT filter effective in removing bacterial and viral pathogens from water (189). Bacterial retention and inactivation is hypothesized to occur on the surface of the filter, whereas log viral removal is proportional to the filter thickness indicating a depth-filtration mechanism. This work provides the basis for future development of a hybrid SWNT-ceramic filter resistant to high temperatures and sufficiently durable for repeated reuse in point-of-use water treatment applications (Figure 4). Again, additional strategies for immobilization of nanomaterials must be developed before widespread application of this technology in drinking water treatment.

The difficulty of nanotube immobilization has been partially solved via direct synthesis of MWNTs on the surface of a conventional metal filter for air filtration applications (190). Reduction of the metal filter with high temperature hydrogen gas forms catalytic sites for nanotube growth. Straightforward manipulation of nanotube morphology and filter collection efficiency is achieved by controlling the flow rate of the reducing agent during nanotube synthesis. While filtration removal efficiencies were quantified for inert NaCl particles, further refinement of the filter through nanotube functionalization routes may enable the removal of specific micropollutants from air streams. For instance, the efficacy of oxidized MWNTs for the adsorption of nicotine and tar has been explored for applications in cigarette filters (191).

Carbonaceous Nanomaterials as Antimicrobial Agents

In addition to spawning a suite of novel environmental applications, the unique properties and nanoscale dimensions of fullerenes and nanotubes have raised concern among toxicologists and environmental scientists (192–194). While explicit mechanisms of antimicrobial activity are still under investigation, toxicity may depend upon physiochemical and structural characteristics such as surface chemistry, functional group density, length, residual catalyst contamination, and diameter (195–202). A number of researchers are hoping to exploit these observed antimicrobial properties in environmental and human health applications (27, 201–203). Specific classes of nanomaterials may be applicable for water disinfection (189), medical therapy (204, 205), antimicrobial surface coatings (206), or laboratory techniques in microbiology (207).

Deliberate perturbation of cell membranes is a potent method for pathogen control. Membrane disrupting agents are broad spectrum antibiotics, and physical mechanisms of toxicity do not stimulate antibiotic resistance. Recent work linking *Escherichia coli* K12 toxicity to direct contact with SWNTs suggests that membrane disruption is a leading mechanism of inactivation (201, 202). Novel antimicrobial surface coatings that exploit the inherent vulnerability of bacteria toward CNTs may provide elegant engineering solutions to the challenging problem of bacterial colonization and biofilm development in drinking water systems, medical implant devices, and other submerged surfaces. Work on CNT toxicity toward diverse microbial communities is ongoing (208).

A number of research groups are investigating applications of antimicrobial and antiviral nanoparticles for water treatment and distribution systems. Removal and inactivation of bacteria and viruses on SWNT hybrid filters is referenced above (189). CNTs have also been proposed as scaffolding agents for antimicrobial Ag nanoparticles (209) or semiconducting photocatalysts such as TiO₂ (68).

Pathogen deactivation by fullerol (99) and nC-60 (210) may also be applicable to water and wastewater treatment if hurdles to immobilization and separation of the nanomaterials are surmounted (211). The antiviral activity of fullerols is hypothesized to act through the generation of singlet oxygen in the presence of UV light or superoxide in the presence of both UV and an electron donating molecule (203). Finally, stable nC-60 suspensions exhibited potent antibacterial activity toward physiologically diverse bacteria over a range of environmental conditions (210).

Carbonaceous Nanomaterials for Environmental Sensing

Environmental scientists, engineers, and policy makers face a challenging range of scale in their work. Contaminants expressed in concentrations of parts-per-trillion are correlated to environmental implications expressed in millions of liters of water or billions of people affected. Skepticism often shrouds the potential for nanotechnology's contributions to these large-scale environmental challenges.

Environmental sensing, however, is one application of nanotechnology with potential to bridge this range of scale. Recent endeavors to monitor environmental change through networked sensing systems will inform predictive models and shape future environmental policy. The Water and Environmental Research Systems Network (WATERS Network), for example, plans an integrated sensor network that will link environmental observatories and provide an accessible cache of data for modeling and predicting water quality and quantity (212). Scalability and forecasting at this magnitude will require a suite of precise and flexible sensors.

CNT based sensors offer a number of advantages to existing sensor platforms, and readers are referred to recent critical reviews on this subject (213–218). Chemical, biological, thermal, optical, stress, strain, pressure, and flow sensors draw upon the exceptional electrical conductivity, chemical stability, high surface area, mechanical stiffness, and straightforward functionalization pathways of CNTs to enhance traditional carbon electrode sensor platforms (219). In another application, arrays of aligned MWNTs grown on an SiO₂ substrate serve as anodes in ionization sensors for gas detection (220). The sharp tips of nanotubes facilitate the generation of high electric fields at low voltages, enabling portable, battery operated, and small scale sensors. Detection occurs via electric field decomposition of the sample followed by cathode registration of a unique fingerprint for each gaseous analyte.

The introduction of CNT nanowire sensors constitutes a major breakthrough for the sensor field. Adsorption of charged species to the surface of the CNT modifies the nanotube conductance, thereby establishing a basis for correlation between current fluctuation and analyte composition or concentration. Kong et al. (221) developed gas sensors in which the electrical resistance of semiconducting SWNTs changed by 3 orders of magnitude seconds after exposure to part per million concentrations of NO₂ or NH₃ at room temperature. The fast response time, low detection limits, and high sensitivity are a function of the large and fully exposed surface area of the SWNTs.

The power of the nanowire sensor platform lies in schemes for rational modification to target specific chemical and biological analytes lacking inherent affinity for CNTs (222). Covalent and supramolecular functionalization enables modification with a suite of chemical groups, metals, enzymes, antibodies, DNA molecules, and biological receptors. The environmental monitoring applications of CNT biosensors are extensively reviewed by Wang (113, 223), Rogers (224), and references contained therein. Other environmental applications include health and safety monitoring, infrastructure management, chemical and material efficiency in manufacturing, and cost-effective regulatory platforms.

Monitoring environmental microbial ecology and detecting microbial pathogens are also objectives of biosensor platform research. Some systems utilize direct adsorptive accumulation of nucleic acid or protein targets to the surface of the CNT electrode array for label-free electrical detection of hybridization (225). Others employ the unique conductive properties of the CNT to amplify signal pathways in both recognition and transduction events (226). Many of these systems have achieved attomolar (10⁻¹⁸ M) or zeptomolar (10⁻²¹ M) detection limits, levels which open opportunities for direct detection techniques rather than the PCR-mediated amplification and analysis currently in practice (113). Widely distributed nanobased sensor networks for rapid and sensitive detection of microbes would strengthen domestic security, enhance online response to microbial outbreaks in drinking water systems, extend subsurface monitoring of biodegradation, or capture evolution in microbial communities after environmental perturbation.

Carbonaceous Nanomaterials for Renewable Energy

Worldwide consumption of marketed energy is anticipated to increase by 57% between 2004 and 2030 (227). Concomitant with this growth are increases in fossil fuel emissions, transnational energy transport, and process water consumption. While coal will be the leading market substitute for shortages in oil and natural gas, meeting the long-term energy challenge will require interdisciplinary and transnational collaboration on advances to solar, wind, biological, or low grade heat source utilization technologies.

Though nanomaterials and nanocomposites will find applications across renewable energy sectors, the majority of applications constitute material improvements to secondary components. CNT anodes, for instance, may improve the sensitivity and spatial resolution of radiation counters used in nuclear power plants (228). Symmetric, aligned nanotube membranes, may enable the use of low grade heat through an osmotic heat engine (229). And stronger, lighter materials may yield structural improvements in wind harvesting devices (230).

The greatest potential for carbonaceous nanomaterials to yield fundamental breakthroughs lies in solar energy applications. Current limitations to photovoltaic and photoelectrochemical energy sector growth include affordability, material availability (e.g., indium), and device flexibility (231).

While inexpensive, micrometer scale carbon materials are common in solar energy conversion and storage devices (232), the improved electronic and optical properties of nanotubes and fullerenes enable novel architectures and extended durability (233). The diversity of carbonaceous nanomaterial applications to solar energy collection, storage, and conversion devices has motivated numerous review articles (231, 233–235). This review critically analyzes a small cross-section of these technologies with the intent of highlighting the enabling role of molecular manipulation on the nanoscale.

Photovoltaic devices convert adsorbed photons into electrical charge to power an external circuit. Novel organic solar cell architectures promise efficient and flexible substitutes to conventional designs utilizing inorganic silicon for photocurrent generation (233). Bound electron–hole pairs (231) and short exciton diffusion lengths in organic semiconductor systems, however, constrain the thickness of the acceptor–donor layer in organic solar cells (231). To accommodate these limitations, the active layer is designed with bulk heterojunction architecture (236) to increase the interfacial area and promote charge transport in organic photovoltaic devices (237). Ideally, the chemical properties of the donor and acceptor materials are tuned to achieve complete phase separation within the active layer and a phase segregation length consistent with the exciton diffusion length (238).

Despite thickness limitations, polymeric-fullerene bulk heterojunction donor–acceptor materials (238–240) are low cost and demonstrate excellent charge separation capabilities (231). The organic solar cell accepting material of choice, fullerenes display strong electron accepting, efficient charge transporting, and dense crystal packing properties (238). Optimization strategies have drawn upon the tunable optical, electronic, and chemical properties of fullerene molecules to maximize the range of photovoltaic applications. For instance, select functional groups improve fullerene miscibility during the thin-film casting process while preserving the optical properties of the polymer–fullerene dyad (238). Molecular manipulations also optimize the HOMO–LUMO energy relationship with the donating polymer, increase the lifespan of the charge separated state, enhance adsorption in the visible light range, and ensure thermodynamically favorable heterojunction morphologies (241). Organic–inorganic hybrid photovoltaic cells and dye-sensitized solar cells (DSSC) have also utilized the optical activity of CNTs and fullerenes as a chromophore (231, 233, 234, 242–247).

Other photovoltaic architectures incorporate carbon-based nanomaterials as a transparent conducting anode. Solar cell efficiency depends on anodes with high optical transmittance to maximize excitation of the active layers and low sheet resistance to reduce power loss. Indium–tin oxide, the conventional material of choice, is environmentally scarce and suffers some chemical and optical limitations (248). Thin films of SWNTs have been explored as a low cost, transparent, highly conductive, and physically flexible anode replacement (249–253). While reasonably high efficiencies have been achieved, optimization is limited by the difficulty of separating semiconducting and metallic SWNTs.

In photoelectrochemical cells, semiconducting materials generate an electron–hole pair and transfer the charge through a circuit to a counter electrode in contact with a redox couple in the electrolyte solution (254). Semiconducting CNTs undergo charge separation upon exposure to UV light, initiating charge transfer to a solution phase reactant (235, 247). While direct use of CNTs' photoactive properties in photoelectrochemical cells have achieved modest photoconversion efficiencies, semiconducting materials such as TiO₂ are superior catalytic agents. Unfortunately, these

nanoscale inorganics suffer from high charge recombination as the free electron migrates to the electrode surface (255). To reduce rates of charge recombination, CNTs have also been proposed as conductive scaffolds to convey charge to the electrode (256, 257). High conductivity and smooth junctions between the electrode and SWNTs enable this reduction in charge recombination (247). Again, synthesis of monochiral nanotubes would dramatically improve the conduction efficiency of CNT scaffolding.

Proton exchange membrane (PEM) fuel cells harvest the chemical energy in photochemically produced hydrogen to generate electricity without combustion byproducts. Basic PEM architecture consists of an anode for hydrogen molecule dissociation, an electrolyte spacer, and a cathode for oxygen reduction (232). While traditional electrode design has incorporated carbon particles as a porous scaffold (232, 233), ordered carbon nanostructures offer improvements to fuel cell voltage output (258–261). Substitution with CNTs at the anode improves charge transfer (260) and optimizes the triple phase contact layer between the carbon electrode, the noble metal catalyst, and the proton conductor (261). At the highly acidic cathode, CNTs' low percentage of dangling bonds enhance corrosion resistance, whereas the porous structure of the CNT mesh electrodes ensures gas diffusivity and a path for water removal (233, 262, 263). When SWNTs are employed as a scaffolding agent, platinum recrystallization rates were also decreased, thereby lengthening the lifespan of the fuel cell (69). Finally, the structural and mechanical properties of CNTs open the possibility for freestanding fuel cell electrodes with enhanced conductivity and ease of fabrication in comparison to nanotubes cast on carbon paper or other support materials (233).

Renewable energy infrastructure also requires efficient and cost-effective energy storage devices. The promise of the hydrogen economy, in particular, depends upon hydrogen storage devices with high storage capacity and rapid desorption under moderate temperature increases. While carbon-based nanomaterials were promoted as the missing link in the fabrication of a robust and inexpensive hydrogen storage system (264), current research (265–269) suggests that existing carbon nanostructures do not satisfy U.S. Department of Energy (DOE) targets (270) for volumetric or gravimetric densities of hydrogen storage. A number of theoretical carbon nanoparticle morphologies have also been modeled (266), though none of the structures yielded hypothetical storage capacities capable of meeting DOE standards. Instead, CNTs are likely to be used as scaffolding agents for metal oxide nanoparticles with high hydrogen affinities (70, 134, 271–276).

Pollution Prevention through Molecular Manipulation

The present review has covered environmental applications insofar as nanomaterials are directly applied toward challenges faced by environmental scientists, engineers, and policy makers. Contaminant remediation, water treatment, sensing, and energy storage each represent product phase environmental applications of nanotechnology. Those who embrace the concepts of life-cycle assessment, however, recognize that the use phase constitutes only a fraction of a technology's evolution from design through disposal. Green chemistry, green engineering, life-cycle design, and industrial ecology probe other phases of product life-cycles for opportunities to minimize environmental impact. Indirect applications of carbonaceous nanomaterials are poised to make significant contributions in these alternate phases of technological development.

Carbon-based nanomaterials enable a suite of composite materials with improved performance characteristics. When

enhanced durability, high strength/weight ratios, or reuse applications of a material are incorporated into product design, the potential exists for products with a longer lifespan and greater material efficiency. Replacing current structural materials with high strength nanotube composites, for instance, could reduce the volume of concrete (277) or the mass of high strength steels (278). Minimization of material flows across life-cycle phases will be a major contribution of nanotechnology to the field of green design.

The contributions that nanomaterials make toward reduced material flow must not be "undone" by resource intensive or environmentally hazardous techniques for synthesizing CNTs. Greener synthesis pathways, solvent substitution in purification techniques, and bottom up manufacturing schemes are being explored to reduce the environmental burden of the nanomaterials themselves (279, 280).

Carbonaceous nanomaterials may also affect the efficiency of manufacturing processes, with nanotubes serving as catalysts, scaffolds for reagents, or when incorporated in membranes, as a nanofluidics applicator of process solutions. Styrene synthesis using CNTs as a replacement for conventional iron-oxide catalysts converted the reaction from endothermic to exothermic, reduced the temperature of reaction by 200 °C, and improved the selectivity of the reaction (281). This process yields a net energy savings of nearly 50% and reduces heavy metal emissions by 75% (281). Commercially viable and alternative energy sources, such as solar cells incorporating SWNT hybrid molecules (282), may eventually power manufacturing facilities and reduce the share of greenhouse gas emissions generated by industrial manufacturing.

Despite the significant pollution prevention opportunities carbonaceous nanotechnologies present in manufacturing and end-of-life stages, product phase applications are likely to drive incorporation of nanotubes and fullerenes into consumer goods. Pending significant toxicological findings, the inherent bias that designers and consumers, alike, hold for product phase applications of a technology will accelerate and focus development of nanotechnology in this direction. In addition to enhanced performance characteristics, a number of existing product phase applications of carbonaceous nanotechnologies focus on reducing energy demands, increasing safety, or enabling component reuse. For example, CNT field emitter displays offer energy and material savings over conventional cathode-ray tube, liquid crystal, and plasma display panels across the preproduction, production, and use phases (281).

Green nanotechnology should also incorporate end-of-life considerations in product design, manufacturing, and applications development. Opportunities for nanomaterial product regeneration or secondary applications should be explored. Nanomaterial sorbents, for instance, might find secondary use in structural reinforcement or road construction. Finally, green product design must consider disposal and containment strategies to minimize the dispersal of nanomaterials in the environment. This is an area ripe for multidisciplinary collaboration between product engineers, environmental scientists, and toxicologists.

Nevertheless, barriers exist to the realization of pollution prevention practices in nanobased product development, implementation, and life-cycle design. Challenges arise when scaling up technologies from bench to industrial level processes. The quality, consistency, and pricing of carbonaceous nanomaterials are still in flux. Existing waste management infrastructure systems are not designed to accommodate new nanobased products. Studies on the fate, transport, and toxicity of CNTs and fullerenes report conflicting results (194, 197). And, public perceptions of risk are

highly volatile toward unfamiliar technologies (283). Efforts to earn public trust through responsible risk communication outlets are one important component of a comprehensive strategy to reinforce nanotechnology's status as a conduit for pollution prevention and green design.

Acknowledgments

M.S.M. acknowledges generous support from the NSF Graduate Research Fellowship Program (GRFP) and the EPA Science to Achieve Results (STAR) Graduate Fellowship Program. This work was also supported by the National Science Foundation under research grants BES-0646247 and BES-0504258.

Literature Cited

- (1) Martin, C. R.; Kohli, P. The emerging field of nanotube biotechnology. *Nat. Rev. Drug Discovery* **2003**, *2*, 29–37.
- (2) Kam, N. W. S.; O'Connell, M.; Wisdom, J. A.; Dai, H. J. Carbon nanotubes as multifunctional biological transporters and near-infrared agents for selective cancer cell destruction. *Proc. Nat. Acad. Sci. U. S. A.* **2005**, *102*, 11600–11605.
- (3) Lopez, C. F.; Nielsen, S. O.; Moore, P. B.; Klein, M. L. Understanding nature's design for a nanosyringe. *Proc. Nat. Acad. Sci. U. S. A.* **2004**, *101*, 4431–4434.
- (4) Tenne, R. Inorganic nanotubes and fullerene-like nanoparticles. *Nat. Nanotechnol.* **2006**, *1*, 103–111.
- (5) Ajayan, P. M. Nanotubes from carbon. *Chem. Rev.* **1999**, *99*, 1787–1800.
- (6) Hu, Y.; Shenderova, O.; Brenner, D. Carbon nanostructures: Morphologies and properties. *J. Comput. Theor. Nanosci.* **2007**, *4*, 199–221.
- (7) Falcao, E. H. L.; Wudl, F. Carbon allotropes: beyond graphite and diamond. *J. Chem. Technol. Biotechnol.* **2007**, *82*, 524–531.
- (8) Dresselhaus, M.; Endo, M. Relation of carbon nanotubes to other carbon materials. *Top. Appl. Phys.* **2001**, *80*, 11–28.
- (9) Kroto, H. W. The stability of the fullerenes C-24, C-28, C-32, C-36, C-50, C-60 and C-70. *Nature* **1987**, *329*, 529–531.
- (10) Campbell, E. E. B.; Fowler, P. W.; Mitchell, D.; Zerbetto, F. Increasing cost of pentagon adjacency for larger fullerenes. *Chem. Phys. Lett.* **1996**, *250*, 544–548.
- (11) Taylor, R.; Walton, D. R. M. The chemistry of fullerenes. *Nature* **1993**, *363*, 685–693.
- (12) Johnson, R. D.; Meijer, G.; Bethune, D. S. C-60 has icosahedral symmetry. *J. Am. Chem. Soc.* **1990**, *112*, 8983–8984.
- (13) Johnson, R.; Bethune, D.; Yannoni, C. Fullerene structure and dynamics - A magnetic-resonance potpourri. *Acc. Chem. Res.* **1992**, *25*, 169–175.
- (14) Diederich, F.; Thilgen, C. Covalent fullerene chemistry. *Science* **1996**, *271*, 317–323.
- (15) Lehn, J.-M.; Atwood, J. L.; Davies, J. E. D.; MacNicol, D. D.; Vögtle, F. *Comprehensive Supramolecular Chemistry*; Pergamon: New York, 1996.
- (16) Bonifazi, D.; Enger, O.; Diederich, F. Supramolecular [60] fullerene chemistry on surfaces. *Chem. Soc. Rev.* **2007**, *36*, 390–414.
- (17) Diederich, F.; Gomez-Lopez, M. Supramolecular fullerene chemistry. *Chem. Soc. Rev.* **1999**, *28*, 263–277.
- (18) Moriarty, P. Nanostructured materials. *Rep. Prog. Phys.* **2001**, *64*, 297–381.
- (19) Kroto, H. W.; Heath, J. R.; O'Brien, S. C.; Curl, R. F.; Smalley, R. E. C-60 - Buckminsterfullerene. *Nature* **1985**, *318*, 162–163.
- (20) Bethune, D. S.; Johnson, R. D.; Salem, J. R.; Devries, M. S.; Yannoni, C. S. Atoms in carbon cages - The structure and properties of endohedral fullerenes. *Nature* **1993**, *366*, 123–128.
- (21) Kessler, B.; Bringer, A.; Cramm, S.; Schlebusch, C.; Eberhardt, W.; Suzuki, S.; Achiba, Y.; Esch, F.; Barnaba, M.; Cocco, D. Evidence for incomplete charge transfer and la-derived states in the valence bands of endohedrally doped La@C-82. *Phys. Rev. Lett.* **1997**, *79*, 2289–2292.
- (22) Shinohara, H.; Sato, H.; Saito, Y.; Takayama, M.; Izuoka, A.; Sugawara, T. Formation and extraction of very large all-carbon fullerenes. *J. Phys. Chem.* **1991**, *95*, 8449–8451.
- (23) Wang, B. C.; Wang, H. W.; Chang, J. C.; Tso, H. C.; Chou, Y. M. More spherical large fullerenes and multi-layer fullerene cages. *J. Mol. Struct.-Theochem.* **2001**, *540*, 171–176.
- (24) Ugarte, D. Curling and closure of graphitic networks under electron-beam irradiation. *Nature* **1992**, *359*, 707–709.
- (25) Bates, K. R.; Scuseria, G. E. Why are buckyonions round. *Theor. Chem. Acc.* **1998**, *99*, 29–33.

- (26) Stone, A. J.; Wales, D. J. Theoretical studies of icosahedral C₆₀ and some related species. *Chem. Phys. Lett.* **1986**, *128*, 501–503.
- (27) Fortner, J. D.; Lyon, D. Y.; Sayes, C. M.; Boyd, A. M.; Falkner, J. C.; Hotze, E. M.; Alemany, L. B.; Tao, Y. J.; Guo, W.; Ausman, K. D.; Colvin, V. L.; Hughes, J. B. C-60 in water: Nanocrystal formation and microbial response. *Environ. Sci. Technol.* **2005**, *39*, 4307–4316.
- (28) Chen, K. L.; Elimelech, M. Aggregation and deposition kinetics of fullerene (C₆₀) nanoparticles. *Langmuir* **2006**, *22*, 10994–11001.
- (29) Scrivens, W. A.; Tour, J. M.; Creek, K. E.; Pirisi, L. Synthesis of 14C-Labeled C₆₀, its suspension in water, and its uptake by human keratinocytes. *J. Am. Chem. Soc.* **1994**, *116*, 4517–4518.
- (30) Andrievsky, G. V.; Kosevich, M. V.; Vovk, O. M.; Shelkovsky, V. S.; Vashchenko, L. A. On the production of an aqueous colloidal solution of fullerenes. *J. Chem. Soc.-Chem. Commun.* **1995**, 1281–1282.
- (31) Duncan, L. K.; Jinschek, J. R.; Vikesland, P. J. C-60 colloid formation in aqueous systems: Effects of preparation method on size, structure, and surface charge. *Environ. Sci. Technol.* **2008**, *42*, 173–178.
- (32) Brant, J. A.; Labille, J.; Bottero, J. Y.; Wiesner, M. R. Characterizing the impact of preparation method on fullerene cluster structure and chemistry. *Langmuir* **2006**, *22*, 3878–3885.
- (33) Brant, J.; Lecoaet, H.; Hotze, M.; Wiesner, M. Comparison of electrokinetic properties of colloidal fullerenes (n-C₆₀) formed using two procedures. *Environ. Sci. Technol.* **2005**, *39*, 6343–6351.
- (34) Chen, K. L.; Elimelech, M. Influence of humic acid on the aggregation kinetics of fullerene C₆₀ nanoparticles in monovalent and divalent electrolyte solutions. *J. Colloid Interface Sci.* **2007**, *309*, 126–34.
- (35) Iijima, S. Helical microtubules of graphitic carbon. *Nature* **1991**, *354*, 56–58.
- (36) Xia, Y. N.; Yang, P. D.; Sun, Y. G.; Wu, Y. Y.; Mayers, B.; Gates, B.; Yin, Y. D.; Kim, F.; Yan, Y. Q. One-dimensional nanostructures: Synthesis, characterization, and applications. *Adv. Mater.* **2003**, *15*, 353–389.
- (37) Hu, J. T.; Odom, T. W.; Lieber, C. M. Chemistry and physics in one dimension: Synthesis and properties of nanowires and nanotubes. *Acc. Chem. Res.* **1999**, *32*, 435–445.
- (38) *Carbon Nanotubes: Synthesis, Structure, Properties, And Applications*; Dresselhaus, M. S., Ed.; Springer: Berlin, NY, 2001; Vol. 80.
- (39) Saito, R.; Fujita, M.; Dresselhaus, G.; Dresselhaus, M. S. Electronic-structure of chiral graphene tubules. *Appl. Phys. Lett.* **1992**, *60*, 2204–2206.
- (40) Bandow, S.; Takizawa, M.; Hirahara, K.; Yudasaka, M.; Iijima, S. Raman scattering study of double-wall carbon nanotubes derived from the chains of fullerenes in single-wall carbon nanotubes. *Chem. Phys. Lett.* **2001**, *337*, 48–54.
- (41) Thess, A.; Lee, R.; Nikolaev, P.; Dai, H. J.; Petit, P.; Robert, J.; Xu, C. H.; Lee, Y. H.; Kim, S. G.; Rinzler, A. G.; Colbert, D. T.; Scuseria, G. E.; Tomanek, D.; Fischer, J. E.; Smalley, R. E. Crystalline ropes of metallic carbon nanotubes. *Science* **1996**, *273*, 483–487.
- (42) Liu, Y. Q.; Gao, L.; Zheng, S.; Wang, Y.; Sun, J.; Kajiura, H.; Li, Y.; Noda, K. Debundling of single-walled carbon nanotubes by using natural polyelectrolytes. *Nanotechnology* **2007**, *18*, 365702.
- (43) Nish, A.; Hwang, J.-Y.; Doig, J.; Nicholas, R. J. Highly selective dispersion of single-walled carbon nanotubes using aromatic polymers. *Nat. Nanotechnol.* **2007**, *2*, 640–646.
- (44) Jin, H.; Jeng, E. S.; Heller, D. A.; Jena, P. V.; Kirmse, R.; Langowski, J.; Strano, M. S. Divalent ion and thermally induced DNA conformational polymorphism on single-walled carbon nanotubes. *Macromolecules* **2007**, *40*, 6731–6739.
- (45) Sun, Y. P.; Fu, K. F.; Lin, Y.; Huang, W. J. Functionalized carbon nanotubes: Properties and applications. *Acc. Chem. Res.* **2002**, *35*, 1096–1104.
- (46) Holzinger, M.; Vostrowsky, O.; Hirsch, A.; Hennrich, F.; Kappes, M.; Weiss, R.; Jellen, F. Sidewall Functionalization of Carbon Nanotubes. *Angew. Chem., Int. Ed.* **2001**, *40*, 4002–4005.
- (47) Andreas, H. Functionalization of single-walled carbon nanotubes. *Angew. Chem., Int. Ed.* **2002**, *41*, 1853–1859.
- (48) Georgakilas, V.; Kordatos, K.; Prato, M.; Guldi, D. M.; Holzinger, M.; Hirsch, A. Organic functionalization of carbon nanotubes. *J. Am. Chem. Soc.* **2002**, *124*, 760–761.
- (49) Banerjee, S.; Hemraj-Benny, T.; Wong, S. S. Covalent surface chemistry of single-walled carbon nanotubes. *Adv. Mater.* **2005**, *17*, 17–29.
- (50) Niyogi, S.; Hamon, M. A.; Hu, H.; Zhao, B.; Bhowmik, P.; Sen, R.; Itkis, M. E.; Haddon, R. C. Chemistry of single-walled carbon nanotubes. *Acc. Chem. Res.* **2002**, *35*, 1105–1113.
- (51) Bahr, J. L.; Tour, J. M. Covalent chemistry of single-wall carbon nanotubes. *J. Mater. Chem.* **2002**, *12*, 1952–1958.
- (52) Chiang, I. W.; Brinson, B. E.; Smalley, R. E.; Margrave, J. L.; Hauge, R. H. Purification and characterization of single-wall carbon nanotubes. *J. Phys. Chem. B* **2001**, *105*, 1157–1161.
- (53) Shelimov, K. B.; Esenaliev, R. O.; Rinzler, A. G.; Huffman, C. B.; Smalley, R. E. Purification of single-wall carbon nanotubes by ultrasonically assisted filtration. *Chem. Phys. Lett.* **1998**, *282*, 429–434.
- (54) Shi, Z. J.; Lian, Y. F.; Liao, F. H.; Zhou, X. H.; Gu, Z. N.; Zhang, Y. G.; Iijima, S. Purification of single-wall carbon nanotubes. *Solid State Commun.* **1999**, *112*, 35–37.
- (55) Plata, D. L.; Gschwend, P. M.; Reddy, C. M. Industrially synthesized single-walled carbon nanotubes: compositional data for users, environmental risk assessments, and source apportionment. *Nanotechnology* **2008**, *19*, 185706.
- (56) Bandow, S.; Asaka, S.; Saito, Y.; Rao, A.; Grigorian, L.; Richter, E.; Eklund, P. Effect of the growth temperature on the diameter distribution and chirality of single-wall carbon nanotubes. *Phys. Rev. Lett.* **1998**, *80*, 3779–3782.
- (57) Cassell, A. M.; Raymakers, J. A.; Kong, J.; Dai, H. J. Large scale CVD synthesis of single-walled carbon nanotubes. *J. Phys. Chem. B* **1999**, *103*, 6484–6492.
- (58) Jost, O.; Gorbunov, A.; Liu, X. J.; Pompe, W.; Fink, J. Single-walled carbon nanotube diameter. *J. Nanosci. Nanotechnol.* **2004**, *4*, 433–440.
- (59) Popov, V. N. Carbon nanotubes: properties and application. *Mater. Sci. Eng., R* **2004**, *43*, 61–102.
- (60) Han, W.; Fan, S.; Li, Q.; Hu, Y. Synthesis of gallium nitride nanorods through a carbon nanotube-confined reaction. *Science* **1997**, *277*, 1287–1289.
- (61) Holt, J.; Park, H.; Wang, Y.; Stadermann, M.; Artyukhin, A.; Grigoropoulos, C.; Noy, A.; Bakajin, O. Fast mass transport through sub-2-nanometer carbon nanotubes. *Science* **2006**, *312*, 1034–1037.
- (62) Rinzler, A. G.; Liu, J.; Dai, H.; Nikolaev, P.; Huffman, C. B.; Rodriguez-Macias, F. J.; Boul, P. J.; Lu, A. H.; Heymann, D.; Colbert, D. T.; Lee, R. S.; Fischer, J. E.; Rao, A. M.; Eklund, P. C.; Smalley, R. E. Large-scale purification of single-wall carbon nanotubes: process, product, and characterization. *Appl. Phys. A: Mater. Sci. Process.* **1998**, *67*, 29–37.
- (63) Bauer, L. A.; Birenbaum, N. S.; Meyer, G. J. Biological applications of high aspect ratio nanoparticles. *J. Mater. Chem.* **2004**, *14*, 517–526.
- (64) Hafner, J. H.; Cheung, C. L.; Woolley, A. T.; Lieber, C. M. Structural and functional imaging with carbon nanotube AFM probes. *Prog. Biophys. Mol. Biol.* **2001**, *77*, 73–110.
- (65) Jin, C. H.; Suenaga, K.; Iijima, S. Plumbing carbon nanotubes. *Nat. Nanotechnol.* **2008**, *3*, 17–21.
- (66) Hunter, R. J., *Foundations of Colloid Science*, 2nd ed.; Oxford University Press: Oxford; New York, 2001.
- (67) Lin, Y. H.; Cui, X. L.; Bontha, J. Electrically controlled anion exchange based on polypyrrole and carbon nanotubes nanocomposite for perchlorate removal. *Environ. Sci. Technol.* **2006**, *40*, 4004–4009.
- (68) Krishna, V.; Pumprueg, S.; Lee, S. H.; Zhao, J.; Sigmund (68) Krishna, V.; Pumprueg, S.; Lee, S. H.; Zhao, J.; Sigmund, W.; Koopman, B.; Moudgil, B. M. Photocatalytic disinfection with titanium dioxide coated multi-wall carbon nanotubes. *Process Saf. Environ. Prot.* **2005**, *83*, 393–397.
- (69) Kongkanand, A.; Kuwabata, S.; Girishkumar, G.; Kamat, P. Single-wall carbon nanotubes supported platinum nanoparticles with improved electrocatalytic activity for oxygen reduction reaction. *Langmuir* **2006**, *22*, 2392–2396.
- (70) Anson, A.; Lafuente, E.; Urriolabeitia, E.; Navarro, R.; Benito, A. M.; Maser, W. K.; Martinez, M. T. Hydrogen capacity of palladium-loaded carbon materials. *J. Phys. Chem. B* **2006**, *110*, 6643–6648.
- (71) Koblinski, P.; Nayak, S. K.; Zapol, P.; Ajayan, P. M. Charge distribution and stability of charged carbon nanotubes. *Phys. Rev. Lett.* **2002**, *89*, 255503.
- (72) Furmaniak, S.; Terzyk, A. P.; Gauden, P. A.; Rychlicki, G. Simple models of adsorption in nanotubes. *J. Colloid Interface Sci.* **2006**, *295*, 310–317.
- (73) Walther, J. H.; Jaffe, R. L.; Kotsalis, E. M.; Werder, T.; Halicioglu, T.; Koumoutsakos, P. Hydrophobic hydration of C-60 and carbon nanotubes in water. *Carbon* **2004**, *42*, 1185–1194.

- (74) Ham, H. T.; Choi, Y. S.; Chung, I. J. An explanation of dispersion states of single-walled carbon nanotubes in solvents and aqueous surfactant solutions using solubility parameters. *J. Colloid Interface Sci.* **2005**, *286*, 216–223.
- (75) Fernandez, A. What caliber pore is like a pipe? Nanotubes as modulators of ionic gradients. *J. Chem. Phys.* **2003**, *119*, 5315–5319.
- (76) Girifalco, L. A.; Hodak, M.; Lee, R. S. Carbon nanotubes, buckyballs, ropes, and a universal graphitic potential. *Phys. Rev. B* **2000**, *62*, 13104–13110.
- (77) Girifalco, L. A. Interaction potential for C60 molecules. *J. Phys. Chem.* **1991**, *95*, 5370–5371.
- (78) Terashima, M.; Nagao, S. Solubilization of [60]fullerene in water by aquatic humic substances. *Chem. Lett.* **2007**, *36*, 302–303.
- (79) Hummer, G.; Rasaiah, J.; Noworyta, J. Water conduction through the hydrophobic channel of a carbon nanotube. *Nature* **2001**, *414*, 188–190.
- (80) Walther, J. H.; Jaffe, R.; Halicioglu, T.; Koumoutsakos, P. Carbon nanotubes in water: Structural characteristics and energetics. *J. Phys. Chem. B* **2001**, *105*, 9980–9987.
- (81) Pederson, M.; Broughton, J. Nanocapillarity in fullerene tubules. *Phys. Rev. Lett.* **1992**, *69*, 2689–2692.
- (82) Dujardin, E.; Ebbesen, T. W.; Hiura, H.; Tanigaki, K. Capillarity and wetting of carbon nanotubes. *Science* **1994**, *265*, 1850–1852.
- (83) Dujardin, E.; Ebbesen, T. W.; Krishnan, A.; Treacy, M. M. J. Wetting of Single Shell Carbon Nanotubes. *Adv. Mater.* **1998**, *10*, 1472–1475.
- (84) Béguin, F.; Flahaut, E.; Linares-Solano, A.; Pinson, J. *Understanding Carbon Nanotubes* **2006**, 495.
- (85) Hilding, J.; Grulke, E. A.; Sinnott, S. B.; Qian, D.; Andrews, R.; Jagtoyen, M. Sorption of butane on carbon multiwall nanotubes at room temperature. *Langmuir* **2001**, *17*, 7540–7544.
- (86) Chen, W.; Duan, L.; Zhu, D. Q. Adsorption of polar and nonpolar organic chemicals to carbon nanotubes. *Environ. Sci. Technol.* **2007**, *41*, 8295–8300.
- (87) Maddox, M. W.; Gubbins, K. E. Molecular simulation of fluid adsorption in buckytubes. *Langmuir* **1995**, *11*, 3988–3996.
- (88) Inoue, S.; Ichikuni, N.; Suzuki, T.; Uematsu, T.; Kaneko, K. Capillary condensation of N₂ on multiwall carbon nanotubes. *J. Phys. Chem. B* **1998**, *102*, 4689–4692.
- (89) Li, Z.; Pan, Z.; Dai, S. Nitrogen adsorption characterization of aligned multiwalled carbon nanotubes and their acid modification. *J. Colloid Interface Sci.* **2004**, *277*, 35–42.
- (90) Avouris, P. Carbon nanotube electronics. *Chem. Phys.* **2002**, *281*, 429–445.
- (91) Kamat, P. V.; Haria, M.; Hotchandani, S. C60 Cluster as an electron shuttle in a Ru(II)-polypyridyl sensitizer-based photochemical solar cell. *J. Phys. Chem. B* **2004**, *108*, 5166–5170.
- (92) Bonchio, M.; Carraro, M.; Scorrano, G.; Bagnò, A. Photooxidation in water by new hybrid molecular photocatalysts integrating an organic sensitizer with a polyoxometalate core. *Adv. Synth. Catal.* **2004**, *346*, 648–654.
- (93) Zhu, S. B.; Xu, T. G.; Fu, H. B.; Zhao, J. C.; Zhu, Y. F. Synergetic effect of Bi₂WO₆ photocatalyst with C-60 and enhanced photoactivity under visible irradiation. *Environ. Sci. Technol.* **2007**, *41*, 6234–6239.
- (94) Narita, M.; Amano, F.; Kadoishi, Y.; Nishiumi, H. Phenol decomposition by visible light catalysis with fullerene. *Kagaku Kagaku Ronbunshu* **2007**, *33*, 564–569.
- (95) Colvin, V. L. Clean Water from Small Materials, In *Nanotechnology in the Environment* MRS: Boston, MA, 2007.
- (96) Ebbesen, T. W.; Tanigaki, K.; Kuroshima, S. Excited-state properties of C60. *Chem. Phys. Lett.* **1991**, *181*, 501–504.
- (97) Lee, J.; Fortner, J. D.; Hughes, J. B.; Kim, J. H. Photochemical production of reactive oxygen species by C-60 in the aqueous phase during UV irradiation. *Environ. Sci. Technol.* **2007**, *41*, 2529–2535.
- (98) Hotze, E. M.; Labille, J.; Alvarez, P.; Wiesner, M. R. Mechanisms of photochemistry and reactive oxygen production by fullerene suspensions in water. *Environ. Sci. Technol.* **2008**, *42*, 4175–4180.
- (99) Pickering, K. D.; Wiesner, M. R. Fullerol-sensitized production of reactive oxygen species in aqueous solution. *Environ. Sci. Technol.* **2005**, *39*, 1359–1365.
- (100) Kamat, J. P.; Devasagayam, T. P. A.; Priyadarsini, K. I.; Mohan, H. Reactive oxygen species mediated membrane damage induced by fullerene derivatives and its possible biological implications. *Toxicology* **2000**, *155*, 55–61.
- (101) Saito, Y.; Uemura, S. Field emission from carbon nanotubes and its application to electron sources. *Carbon* **2000**, *38*, 169–182.
- (102) Hamada, N.; Sawada, S.-i.; Oshiyama, A. New one-dimensional conductors: Graphitic microtubules. *Phys. Rev. Lett.* **1992**, *68*, 1579–1581.
- (103) Ebbesen, T. W.; Lezec, H. J.; Hiura, H.; Bennett, J. W.; Ghaemi, H. F.; Thio, T. Electrical conductivity of individual carbon nanotubes. *Nature* **1996**, *382*, 54–56.
- (104) Tans, S. J.; Devoret, M. H.; Dai, H.; Thess, A.; Smalley, R. E.; Geerligs, L. J.; Dekker, C. Individual single-wall carbon nanotubes as quantum wires. *Nature* **1997**, *386*, 474–477.
- (105) Langer, L.; Bayot, V.; Grivei, E.; Issi, J. P.; Heremans, J. P.; Olk, C. H.; Stockman, L.; Van Haesendonck, C.; Bruynseraede, Y. Quantum transport in a multiwalled carbon nanotube. *Phys. Rev. Lett.* **1996**, *76*, 479–482.
- (106) Bockrath, M.; Cobden, D. H.; McEuen, P. L.; Chopra, N. G.; Zettl, A.; Thess, A.; Smalley, R. E. Single-electron transport in ropes of carbon nanotubes. *Science* **1997**, *275*, 1922–1925.
- (107) Lee, R. S.; Kim, H. J.; Fischer, J. E.; Thess, A.; Smalley, R. E. Conductivity enhancement in single-walled carbon nanotube bundles doped with K and Br. *Nature* **1997**, *388*, 255–257.
- (108) Rao, A. M.; Eklund, P. C.; Bandow, S.; Thess, A.; Smalley, R. E. Evidence for charge transfer in doped carbon nanotube bundles from Raman scattering. *Nature* **1997**, *388*, 257–259.
- (109) Carroll, D. L.; Redlich, P.; Blase, X.; Charlier, J. C.; Curran, S.; Ajayan, P. M.; Roth, S.; Ruhle, M. Effects of nanodomain formation on the electronic structure of doped carbon nanotubes. *Phys. Rev. Lett.* **1998**, *81*, 2332–2335.
- (110) Lim, T. C.; Ramakrishna, S. A conceptual review of nanosensors. *Z. Naturforsch., A: Phys. Sci.* **2006**, *61*, 402–412.
- (111) Pejčić, B.; Eadington, P.; Ross, A. Environmental monitoring of hydrocarbons: Sensor perspective a chemical. *Environ. Sci. Technol.* **2007**, *41*, 6333–6342.
- (112) Sinha, N.; Ma, J. Z.; Yeow, J. T. W. Carbon nanotube-based sensors. *J. Nanosci. Nanotechnol.* **2006**, *6*, 573–590.
- (113) Wang, J. Carbon-nanotube based electrochemical biosensors: A review. *Electroanalysis* **2005**, *17*, 7–14.
- (114) Maiti, A.; andzelm, J.; Tanpipat, N.; von Allmen, P. Effect of adsorbates on field emission from carbon nanotubes. *Phys. Rev. Lett.* **2001**, *87*, 155502.
- (115) Berber, S.; Kwon, Y. K.; Tomanek, D. Unusually high thermal conductivity of carbon nanotubes. *Phys. Rev. Lett.* **2000**, *84*, 4613–4616.
- (116) Kim, P.; Shi, L.; Majumdar, A.; McEuen, P. L. Thermal transport measurements of individual multiwalled nanotubes. *Phys. Rev. Lett.* **2001**, *87*, 215502.
- (117) Cahill, D. G.; Ford, W. K.; Goodson, K. E.; Mahan, G. D.; Majumdar, A.; Maris, H. J.; Merlin, R.; Phillpot, S. R. Nanoscale thermal transport. *J. Appl. Phys.* **2003**, *93*, 793–818.
- (118) Pignatello, J. J.; Xing, B. S. Mechanisms of slow sorption of organic chemicals to natural particles. *Environ. Sci. Technol.* **1996**, *30*, 1–11.
- (119) Allen-King, R. M.; Grathwohl, P.; Ball, W. P. New modeling paradigms for the sorption of hydrophobic organic chemicals to heterogeneous carbonaceous matter in soils, sediments, and rocks. *Adv. Water Resour.* **2002**, *25*, 985–1016.
- (120) Bailey, S. E.; Olin, T. J.; Bricka, R. M.; Adrian, D. D. A review of potentially low-cost sorbents for heavy metals. *Water Res.* **1999**, *33*, 2469–2479.
- (121) Luthy, R. G.; Aiken, G. R.; Brusseau, M. L.; Cunningham, S. D.; Gschwend, P. M.; Pignatello, J. J.; Reinhard, M.; Traina, S. J.; Weber, W. J.; Westall, J. C. Sequestration of hydrophobic organic contaminants by geosorbents. *Environ. Sci. Technol.* **1997**, *31*, 3341–3347.
- (122) Weber, W. J.; McGinley, P. M.; Katz, L. E. Sorption phenomena in subsurface systems—Concepts, models and effects on contaminant fate and transport. *Water Res.* **1991**, *25*, 499–528.
- (123) Schwarzenbach, R. P.; Westall, J. Transport of non-polar organic-compounds from surface-water to groundwater - Laboratory sorption studies. *Environ. Sci. Technol.* **1981**, *15*, 1360–1367.
- (124) Lu, C. S.; Chung, Y. L.; Chang, K. F. Adsorption of trihalomethanes from water with carbon nanotubes. *Water Res.* **2005**, *39*, 1183–1189.
- (125) Yang, K.; Wang, X. L.; Zhu, L. Z.; Xing, B. S. Competitive sorption of pyrene, phenanthrene, and naphthalene on multiwalled carbon nanotubes. *Environ. Sci. Technol.* **2006**, *40*, 5804–5810.
- (126) Yang, K.; Zhu, L. Z.; Xing, B. S. Adsorption of polycyclic aromatic hydrocarbons by carbon nanomaterials. *Environ. Sci. Technol.* **2006**, *40*, 1855–1861.
- (127) Cheng, X. K.; Kan, A. T.; Tomson, M. B. Uptake and sequestration of naphthalene and 1,2-dichlorobenzene by C-60. *Journal of Nanopart. Res.* **2005**, *7*, 555–567.

- (128) Cheng, X. K.; Kan, A. T.; Tomson, M. B. Naphthalene adsorption and desorption from aqueous C-60 fullerene. *J. Chem. Eng. Data* **2004**, *49*, 675–683.
- (129) Cai, Y. Q.; Jiang, G. B.; Liu, J. F.; Zhou, Q. X. Multiwalled carbon nanotubes as a solid-phase extraction adsorbent for the determination of bisphenol a, 4-n-nonylphenol, and 4-tert-octylphenol. *Anal. Chem.* **2003**, *75*, 2517–2521.
- (130) Long, R. Q.; Yang, R. T. Carbon nanotubes as superior sorbent for dioxin removal. *J. Am. Chem. Soc.* **2001**, *123*, 2058–2059.
- (131) Gotovac, S.; Hattori, Y.; Noguchi, D.; Miyamoto, J.; Kanamaru, M.; Utsumi, S.; Kanoh, H.; Kaneko, K. Phenanthrene adsorption from solution on single wall carbon nanotubes. *J. Phys. Chem. B* **2006**, *110*, 16219–16224.
- (132) Papirer, E.; Brendle, E.; Ozil, F.; Balard, H. Comparison of the surface properties of graphite, carbon black and fullerene samples, measured by inverse gas chromatography. *Carbon* **1999**, *37*, 1265–1274.
- (133) Peng, X. J.; Li, Y. H.; Luan, Z. K.; Di, Z. C.; Wang, H. Y.; Tian, B. H.; Jia, Z. P. Adsorption of 1,2-dichlorobenzene from water to carbon nanotubes. *Chem. Phys. Lett.* **2003**, *376*, 154–158.
- (134) Yang, F. H.; Lachawiec, A. J.; Yang, R. T. Adsorption of spillover hydrogen atoms on single-wall carbon nanotubes. *J. Phys. Chem. B* **2006**, *110*, 6236–6244.
- (135) Yang, K.; Xing, B. S. Desorption of polycyclic aromatic hydrocarbons from carbon nanomaterials in water. *Environ. Pollut.* **2007**, *145*, 529–537.
- (136) Neimark, A. V.; Ruetsch, S.; Kornev, K. G.; Ravikovitch, P. I. Hierarchical pore structure and wetting properties of single-wall carbon nanotube fibers. *Nano Letters* **2003**, *3*, 419–423.
- (137) Punyamurtula, V. K.; Qiao, Y. Hysteresis of sorption isotherm of multiwall carbon nanotube in paraxylene. *Mater. Res. Innovations* **2007**, *11*, 37–39.
- (138) Kowalczyk, P.; Holyst, R. Efficient adsorption of super greenhouse gas tetrafluoromethane in carbon nanotubes. *Environ. Sci. Technol.* **2008**, *42*, 2931–2936.
- (139) Savage, N.; Diallo, M. S. Nanomaterials and water purification: Opportunities and challenges. *J. Nanopart. Res.* **2005**, *7*, 331–342.
- (140) Yan, H.; Gong, A. J.; He, H. S.; Zhou, J.; Wei, Y. X.; Lv, L. Adsorption of microcystins by carbon nanotubes. *Chemosphere* **2006**, *62*, 142–148.
- (141) Lecoanet, H. F.; Bottero, J. Y.; Wiesner, M. R. Laboratory assessment of the mobility of nanomaterials in porous media. *Environ. Sci. Technol.* **2004**, *38*, 5164–5169.
- (142) Li, Y.-H.; Wang, S.; Wei, J.; Zhang, X.; Xu, C.; Luan, Z.; Wu, D.; Wei, B. Lead adsorption on carbon nanotubes. *Chem. Phys. Lett.* **2002**, *357*, 263–266.
- (143) Wang, X. K.; Chen, C. L.; Hu, W. P.; Ding, A. P.; Xu, D.; Zhou, X. Sorption of ²⁴³Am(III) to Multiwall Carbon nanotubes. *Environ. Sci. Technol.* **2005**, *39*, 2856–2860.
- (144) Li, Y. H.; Ding, J.; Luan, Z. K.; Di, Z. C.; Zhu, Y. F.; Xu, C. L.; Wu, D. H.; Wei, B. Q. Competitive adsorption of Pb²⁺, Cu²⁺ and Cd²⁺ ions from aqueous solutions by multiwalled carbon nanotubes. *Carbon* **2003**, *41*, 2787–2792.
- (145) Peng, X. J.; Luan, Z. K.; Ding, J.; Di, Z. H.; Li, Y. H.; Tian, B. H. Ceria nanoparticles supported on carbon nanotubes for the removal of arsenate from water. *Mater. Lett.* **2005**, *59*, 399–403.
- (146) Di, Z. C.; Ding, J.; Peng, X. J.; Li, Y. H.; Luan, Z. K.; Liang, J. Chromium adsorption by aligned carbon nanotubes supported ceria nanoparticles. *Chemosphere* **2006**, *62*, 861–865.
- (147) Li, Y.-H.; Wang, S.; Cao, A.; Zhao, D.; Zhang, X.; Xu, C.; Luan, Z.; Ruan, D.; Liang, J.; Wu, D.; Wei, B. Adsorption of fluoride from water by amorphous alumina supported on carbon nanotubes. *Chem. Phys. Lett.* **2001**, *350*, 412–416.
- (148) Lu, C.; Chiu, H.; Bai, H. Comparisons of adsorbent cost for the removal of zinc (II) from aqueous solution by carbon nanotubes and activated carbon. *J. Nanosci. Nanotechnol.* **2007**, *7*, 1647–1652.
- (149) Gallego, M.; Depena, Y. P.; Valcarcel, M. Fullerenes as sorbent materials for metal preconcentration. *Anal. Chem.* **1994**, *66*, 4074–4078.
- (150) Liang, P.; Liu, Y.; Guo, L.; Zeng, J.; Lu, H. B. Multiwalled carbon nanotubes as solid-phase extraction adsorbent for the preconcentration of trace metal ions and their determination by inductively coupled plasma atomic emission spectrometry. *J. Anal. At. Spectrom.* **2004**, *19*, 1489–1492.
- (151) Liu, C.; Fan, Y. Y.; Liu, M.; Cong, H. T.; Cheng, H. M.; Dresselhaus, M. S. Hydrogen storage in single-walled carbon nanotubes at room temperature. *Science* **1999**, *286*, 1127–1129.
- (152) Consales, M.; Crescitelli, A.; Campopiano, S.; Cutolo, A.; Penza, M.; Aversa, P.; Giordano, M.; Cusano, A. Chemical detection in water by single-walled carbon nanotubes-based optical fiber sensors. *IEEE Sens. J.* **2007**, *7*, 1004–1005.
- (153) Shannon, M. A.; Bohn, P. W.; Elimelech, M.; Georgiadis, J. G.; Marinan, B. J.; Mayes, A. M. Science and technology for water purification in the coming decades. *Nature* **2008**, *452*, 301–310.
- (154) Jirage, K. B.; Hulteen, J. C.; Martin, C. R. Nanotubule-based molecular-filtration membranes. *Science* **1997**, *278*, 655–658.
- (155) Majumder, M.; Zhan, X.; Andrews, R.; Hinds, B. J. Voltage gated carbon nanotube membranes. *Langmuir* **2007**, *23*, 8624–8631.
- (156) Majumder, M.; Chopra, N.; Hinds, B. Effect of tip functionalization on transport through vertically oriented carbon nanotube membranes. *J. Am. Chem. Soc.* **2005**, *127*, 9062–9070.
- (157) Nednoor, P.; Chopra, N.; Gavalas, V.; Bachas, L.; Hinds, B. Reversible biochemical switching of ionic transport through aligned carbon nanotube membranes. *Chem. Mater.* **2005**, *17*, 3595–3599.
- (158) Gray, G. T.; McCutcheon, J. R.; Elimelech, M. Internal concentration polarization in forward osmosis: Role of membrane orientation. *Desalination* **2006**, *197*, 1–8.
- (159) McCutcheon, J. R.; Elimelech, M. Modeling water flux in forward osmosis: Implications for improved membrane design. *AIChE J.* **2007**, *53*, 1736–1744.
- (160) McCutcheon, J. R.; McGinnis, R. L.; Elimelech, M. A novel ammonia-carbon dioxide forward direct osmosis desalination process. *Desalination* **2005**, *174*, 1–11.
- (161) Hinds, B.; Chopra, N.; Rantell, T.; Andrews, R.; Gavalas, V.; Bachas, L. Aligned multiwalled carbon nanotube membranes. *Science* **2004**, *303*, 62–65.
- (162) Majumder, M.; Chopra, N.; Andrews, R.; Hinds, B. J. Nanoscale hydrodynamics: Enhanced flow in carbon nanotubes. *Nature* **2005**, *438*, 930.
- (163) Aleksandrov, P. S. *Elementary Concepts of Topology*; Dover Publications: New York, 1961.
- (164) Whitby, M.; Quirke, N. Fluid flow in carbon nanotubes and nanopipes. *Nat. Nanotechnol.* **2007**, *2*, 87–94.
- (165) Mann, D.; Halls, M. Water alignment and proton conduction inside carbon nanotubes. *Phys. Rev. Lett.* **2003**, *90*, 195503.
- (166) Bolhuis, P. G.; Chandler, D. Transition path sampling of cavitation between molecular scale solvophobic surfaces. *J. Chem. Phys.* **2000**, *113*, 8154–8160.
- (167) Barrat, J.-L.; Bocquet, L. Large slip effect at a nonwetting fluid-solid interface. *Phys. Rev. Lett.* **1999**, *82*, 4671–4674.
- (168) Baudry, J.; Charlaix, E.; Tonck, A.; Mazuyer, D. Experimental evidence for a large slip effect at a nonwetting fluid-solid interface. *Langmuir* **2001**, *17*, 5232–5236.
- (169) Kalra, A.; Garde, S.; Hummer, G. Osmotic water transport through carbon nanotube membranes. *Proc. Nat. Acad. Sci. U. S. A.* **2003**, *100*, 10175–10180.
- (170) Sokhan, V.; Nicholson, D.; Quirke, N. Fluid flow in nanopores: Accurate boundary conditions for carbon nanotubes. *J. Chem. Phys.* **2002**, *117*, 8531–8539.
- (171) Joseph, S.; Aluru, N. R. Why are carbon nanotubes fast transporters of water. *Nano Letters* **2008**, *8*, 452–458.
- (172) Kotsalis, E. M.; Walther, J. H.; Koumoutsakos, P. Multiphase water flow inside carbon nanotubes. *Int. J. Multiphase Flow* **2004**, *30*, 995–1010.
- (173) Arora, G.; Sandler, S. I. Molecular sieving using single wall carbon nanotubes. *Nano Letters* **2007**, *7*, 565–569.
- (174) Yeh, I. C.; Hummer, G. Nucleic acid transport through carbon nanotube membranes. *Proc. Nat. Acad. Sci. U. S. A.* **2004**, *101*, 12177–12182.
- (175) Wang, Z.; Ci, L.; Chen, L.; Nayak, S.; Ajayan, P.; Koratkar, N. Polarity-dependent electrochemically controlled transport of water through carbon nanotube membranes. *Nano Letters* **2007**, *7*, 697–702.
- (176) Park, H. G.; Holt, J. K.; Klunder, G.; Grigoropoulos, C. P.; Noy, A.; Bakajin, O., *Ion Exclusion in the Surface-Modified Carbon Nanotube Membranes*; NSTI Nanotech 2007: Santa Clara, CA, 2007.
- (177) Seidel, A.; Waypa, J. J.; Elimelech, M. Role of charge (Donnan) exclusion in removal of arsenic from water by a negatively charged porous nanofiltration membrane. *Environ. Eng. Sci.* **2001**, *18*, 105–113.
- (178) Carrillo-Tripp, M.; San-Roman, M. L.; Hernandez-Cobos, J.; Saint-Martin, H.; Ortega-Blake, I. Ion hydration in nanopores and the molecular basis of selectivity. *Biophys. Chem.* **2006**, *124*, 243–250.

- (179) Tansel, B.; Sager, J.; Rector, T.; Garland, J.; Strayer, R. F.; Levine, L. F.; Roberts, M.; Hummerick, M.; Bauer, J. Significance of hydrated radius and hydration shells on ionic permeability during nanofiltration in dead end and cross flow modes. *Sep. Purif. Technol.* **2006**, *51*, 40–47.
- (180) Wang, Z.; Ci, L.; Chen, L.; Nayak, S.; Ajayan, P.; Koratkar, N. Polarity-dependent electrochemically controlled transport of water through carbon nanotube membranes. *Nano Letters* **2007**, *7*, 697–702.
- (181) Li, J. Y.; Gong, X. J.; Lu, H. J.; Li, D.; Fang, H. P.; Zhou, R. H. Electrostatic gating of a nanometer water channel. *Proc. Nat. Acad. Sci. U. S. A.* **2007**, *104*, 3687–3692.
- (182) Li, X. S.; Zhu, G. Y.; Dordick, J. S.; Ajayan, P. M. Compression-modulated tunable-pore carbon-nanotube membrane filters. *Small* **2007**, *3*, 595–599.
- (183) Cong, H. L.; Zhang, J. M.; Radosz, M.; Shen, Y. Q. Carbon nanotube composite membranes of brominated poly(2,6-diphenyl-1,4-phenylene oxide) for gas separation. *J. Membr. Sci.* **2007**, *294*, 178–185.
- (184) Peng, F. B.; Hu, C. L.; Jiang, Z. Y. Novel ploy(vinyl alcohol)/carbon nanotube hybrid membranes for pervaporation separation of benzene/cyclohexane mixtures. *J. Membr. Sci.* **2007**, *297*, 236–242.
- (185) Choi, J. H.; Jegal, J.; Kim, W. N. Fabrication and characterization of multi-walled carbon nanotubes/polymer blend membranes. *J. Membr. Sci.* **2006**, *284*, 406–415.
- (186) Wang, X.; Chen, X.; Yoon, K.; Fang, D.; Hsiao, B. S.; Chu, B. High flux filtration medium based on nanofibrous substrate with hydrophilic nanocomposite coating. *Environ. Sci. Technol.* **2005**, *39*, 7684–7691.
- (187) Jin, X.; Hu, J. Y.; Tint, M. L.; Ong, S. L.; Biryulin, Y.; Polotskaya, G. Estrogenic compounds removal by fullerene-containing membranes. *Desalination* **2007**, *214*, 83–90.
- (188) Srivastava, A.; Srivastava, O. N.; Talapatra, S.; Vajtai, R.; Ajayan, P. M. Carbon nanotube filters. *Nat. Mater.* **2004**, *3*, 610–614.
- (189) Brady-Estevez, A. S.; Kang, S.; Elimelech, M. A single-walled-carbon-nanotube filter for removal of viral and bacterial pathogens. *Small* **2008**, *4*, 481–484.
- (190) Park, S. J.; Lee, D. G. Performance improvement of micron-sized fibrous metal filters by direct growth of carbon nanotubes. *Carbon* **2006**, *44*, 1930–1935.
- (191) Chen, Z.; Zhang, L.; Tang, Y.; Jia, Z. Adsorption of nicotine and tar from the mainstream smoke of cigarettes by oxidized carbon nanotubes. *Appl. Surf. Sci.* **2006**, *252*, 2933–2937.
- (192) Colvin, V. L. The potential environmental impact of engineered nanomaterials. *Nat. Biotechnol.* **2003**, *21*, 1166–1170.
- (193) Nel, A.; Xia, T.; Madler, L.; Li, N. Toxic potential of materials at the nanolevel. *Science* **2006**, *311*, 622–627.
- (194) Lam, C. W.; James, J. T.; McCluskey, R.; Arepalli, S.; Hunter, R. L. A review of carbon nanotube toxicity and assessment of potential occupational and environmental health risks. *Crit. Rev. Toxicol.* **2006**, *36*, 189–217.
- (195) Jia, G.; Wang, H. F.; Yan, L.; Wang, X.; Pei, R. J.; Yan, T.; Zhao, Y. L.; Guo, X. B. Cytotoxicity of carbon nanomaterials: Single-wall nanotube, multi-wall nanotube, and fullerene. *Environ. Sci. Technol.* **2005**, *39*, 1378–1383.
- (196) Karakoti, A. S.; Hench, L. L.; Seal, S. The potential toxicity of nanomaterials—The role of surfaces. *JOM* **2006**, *58*, 77–82.
- (197) Worle-Knirsch, J. M.; Pulskamp, K.; Krug, H. F. Oops they did it again! Carbon nanotubes hoax scientists in viability assays. *Nano Letters* **2006**, *6*, 1261–1268.
- (198) Sayes, C. M.; Liang, F.; Hudson, J. L.; Mendez, J.; Guo, W. H.; Beach, J. M.; Moore, V. C.; Doyle, C. D.; West, J. L.; Billups, W. E.; Ausman, K. D.; Colvin, V. L. Functionalization density dependence of single-walled carbon nanotubes cytotoxicity in vitro. *Toxicol. Lett.* **2006**, *161*, 135–142.
- (199) Lyon, D. Y.; Adams, L. K.; Falkner, J. C.; Alvarez, P. J. J. Antibacterial activity of fullerene water suspensions: Effects of preparation method and particle size. *Environ. Sci. Technol.* **2006**, *40*, 4360–4366.
- (200) Tang, Y. J.; Ashcroft, J. M.; Chen, D.; Min, G. W.; Kim, C. H.; Murkhejee, B.; Larabell, C.; Keasling, J. D.; Chen, F. Q. F. Charge-associated effects of fullerene derivatives on microbial structural integrity and central metabolism. *Nano Letters* **2007**, *7*, 754–760.
- (201) Kang, S.; Pinault, M.; Pfefferle, L. D.; Elimelech, M. Single-walled carbon nanotubes exhibit strong antimicrobial activity. *Langmuir* **2007**, *23*, 8670–8673.
- (202) Kang, S.; Herzberg, M.; Rodrigues, D. F.; Elimelech, M. Antibacterial effects of carbon nanotubes: Size does matter! *Langmuir* **2008**, *24*, 6409–6413.
- (203) Badireddy, A. R.; Hotze, E. M.; Chellam, S.; Alvarez, P.; Wiesner, M. R. Inactivation of Bacteriophages via photosensitization of fullerol nanoparticles. *Environ. Sci. Technol.* **2007**, *41*, 6627–6632.
- (204) Kim, J. W.; Shashkov, E. V.; Galanzha, E. I.; Kotagiri, N.; Zharov, V. P. Photothermal antimicrobial nanotherapy and nanodiagnosics with self-assembling carbon nanotube clusters. *Lasers Surg. Med.* **2007**, *39*, 622–634.
- (205) Tsao, N.; Luh, T. Y.; Chou, C. K.; Chang, T. Y.; Wu, J. J.; Liu, C. C.; Lei, H. Y. In vitro action of carboxyfullerene. *J. Antimicrob. Chemother.* **2002**, *49*, 641–649.
- (206) Asuri, P.; Karajanagi, S. S.; Kane, R. S.; Dordick, J. S. Polymer-nanotube-enzyme composites as active antifouling films. *Small* **2007**, *3*, 50–53.
- (207) Rojas-Chapana, J.; Troszczyńska, J.; Firkowska, I.; Morsczech, C.; Giersig, M. Multi-walled carbon nanotubes for plasmid delivery into *Escherichia coli* cells. *Lab On A Chip* **2005**, *5*, 536–539.
- (208) Tong, Z. H.; Bischoff, M.; Nies, L.; Applegate, B.; Turco, R. F. Impact of fullerene (C-60) on a soil microbial community. *Environ. Sci. Technol.* **2007**, *41*, 2985–2991.
- (209) Morones, J. R.; Elechiguerra, J. L.; Camacho, A.; Holt, K.; Kouri, J. B.; Ramirez, J. T.; Yacaman, M. J. The bactericidal effect of silver nanoparticles. *Nanotechnology* **2005**, *16*, 2346–2353.
- (210) Lyon, D. Y.; Brown, D. A.; Alvarez, P. J. J. Implications and potential applications of bactericidal fullerene water suspensions: Effect of nC60 concentration, exposure conditions and shelf life. *Water Sci. Technol.* **2008**, *57*, 1533–1538.
- (211) Wiesner, M. R. Responsible development of nanotechnologies for water and wastewater treatment. *Water Sci. Technol.* **2006**, *53*, 45–51.
- (212) WATERS Network Design Team. *WATERS Network Overview Presentation - Transforming Environmental Engineering and Hydrologic Science Research through an Integrated Environmental Observing System*; AEESP Meeting: Virginia Tech, Blacksburg, VA, 2007.
- (213) Valentini, F.; Biagiotti, V.; Lete, C.; Palleschi, G.; Wang, J. The electrochemical detection of ammonia in drinking water based on multi-walled carbon nanotube/copper nanoparticle composite paste electrodes. *Sens. Actuators, B* **2007**, *128*, 326–333.
- (214) Chopra, N.; Gavalas, V. G.; Hinds, B. J.; Bachas, L. G. Functional one-dimensional nanomaterials: Applications in nanoscale biosensors. *Anal. Lett.* **2007**, *40*, 2067–2096.
- (215) Kim, S. N.; Rusling, J. F.; Papadimitrakopoulos, F. Carbon nanotubes for electronic and electrochemical detection of biomolecules. *Adv. Mater.* **2007**, *19*, 3214–3228.
- (216) Hierold, C.; Jungen, A.; Stampfer, C.; Helbling, T. Nano electromechanical sensors based on carbon nanotubes. *Sens. Actuators, A* **2007**, *136*, 51–61.
- (217) Zhao, Q.; Gan, Z. H.; Zhuang, Q. K. Electrochemical sensors based on carbon nanotubes. *Electroanalysis* **2002**, *14*, 1609–1613.
- (218) Allen, B. L.; Kichambare, P. D.; Star, A. Carbon nanotube field-effect-transistor-based biosensors. *Adv. Mater.* **2007**, *19*, 1439–1451.
- (219) Britto, P. J.; Santhanam, K. S. V.; Ajayan, P. M. Carbon nanotube electrode for oxidation of dopamine. *Bioelectrochem. Bioenerg.* **1996**, *41*, 121–125.
- (220) Modi, A.; Koratkar, N.; Lass, E.; Wei, B. Q.; Ajayan, P. M. Miniaturized gas ionization sensors using carbon nanotubes. *Nature* **2003**, *424*, 171–174.
- (221) Kong, J.; Franklin, N. R.; Zhou, C. W.; Chapline, M. G.; Peng, S.; Cho, K. J.; Dai, H. J. Nanotube molecular wires as chemical sensors. *Science* **2000**, *287*, 622–625.
- (222) Kong, J.; Chapline, M. G.; Dai, H. J. Functionalized carbon nanotubes for molecular hydrogen sensors. *Adv. Mater.* **2001**, *13*, 1384–1386.
- (223) Lin, Y. H.; Yantasee, W.; Wang, J. Carbon nanotubes (CNTs) for the development of electrochemical biosensors. *Front. Biosci.* **2005**, *10*, 492–505.
- (224) Rogers, K. R. Recent advances in biosensor techniques for environmental monitoring. *Anal. Chim. Acta* **2006**, *568*, 222–231.
- (225) Koehne, J.; Chen, H.; Li, J.; Cassell, A. M.; Ye, Q.; Ng, H. T.; Han, J.; Meyyappan, M. Ultrasensitive label-free DNA analysis using an electronic chip based on carbon nanotube nanoelectrode arrays. *Nanotechnology* **2003**, *14*, 1239–1245.
- (226) Wang, J.; Liu, G. D.; Jan, M. R. Ultrasensitive electrical biosensing of proteins and DNA: Carbon-nanotube derived amplification of the recognition and transduction events. *J. Am. Chem. Soc.* **2004**, *126*, 3010–3011.

- (227) *International Energy Outlook, U.S.*, DOE/EIA-0484: Department of Energy: Washington, DC, 2007.
- (228) Kotani, T.; Ueno, M.; Kawai, N.; Kitamoto, S. Development of a new radiation detector utilizing carbon nanotube as anode. *Physica E* **2007**, *40*, 422–424.
- (229) McGinnis, R. L.; McCutcheon, J. R.; Elimelech, M. A novel ammonia-carbon dioxide osmotic heat engine for power generation. *J. Membr. Sci.* **2007**, *305*, 13–19.
- (230) Orth, F.; Hoffmann, L.; Zilchbremer, H.; Ehrenstein, G. W. Evaluation of composites under dynamic load. *Compos. Struct.* **1993**, *24*, 265–272.
- (231) Randt, B. P.; Genoe, J.; Herernans, P.; Poortmans, J. Solar cells utilizing small molecular weight organic semiconductors. *Prog. Photovoltaics* **2007**, *15*, 659–676.
- (232) Carrette, L.; Friedrich, K. A.; Stimming, U. Fuel cells: Principles, types, fuels, and applications. *ChemPhysChem* **2000**, *1*, 162–193.
- (233) Mao, S. S.; Chen, X. B. Selected nanotechnologies for renewable energy applications. *Int. J. Energy Res.* **2007**, *31*, 619–636.
- (234) Kamat, P. V. Meeting the clean energy demand: Nanostructure architectures for solar energy conversion. *J. Phys. Chem. C* **2007**, *111*, 2834–2860.
- (235) Guldi, D. M. Biomimetic assemblies of carbon nanostructures for photochemical energy Conversion. *J. of Phys. Chem. B* **2005**, *109*, 11432–11441.
- (236) Halls, J. J. M.; Walsh, C. A.; Greenham, N. C.; Marseglia, E. A.; Friend, R. H.; Moratti, S. C.; Holmes, A. B. Efficient photodiodes from interpenetrating polymer networks. *Nature* **1995**, *376*, 498–500.
- (237) Joël Davenas, P. A. A. L. A. B. Influence of the nanoscale morphology on the photovoltaic properties of fullerene/MEH-PPV composites. *Macromol. Symp.* **2006**, *233*, 203–209.
- (238) Thompson, B. C.; Frechet, J. M. J. Organic photovoltaics - Polymer-fullerene composite solar cells. *Angew. Chem., Int. Ed.* **2008**, *47*, 58–77.
- (239) Janssen, R. A. J.; Hummelen, J. C.; Saricifti, N. S. Polymer-fullerene bulk heterojunction solar cells. *MRS Bulletin* **2005**, *30*, 33–36.
- (240) Li, C.; Mitra, S. Processing of fullerene-single wall carbon nanotube complex for bulk heterojunction photovoltaic cells. *Appl. Phys. Lett.* **2007**, *91*, 253112.
- (241) Koeppel, R.; Saricifti, N. S. Photoinduced charge and energy transfer involving fullerene derivatives. *Photochem. Photobiol. Sci.* **2006**, *5*, 1122–1131.
- (242) Kudo, N.; Shimazaki, Y.; Ohkita, H.; Ohoka, M.; Ito, S. Organic-inorganic hybrid solar cells based on conducting polymer and SnO₂ nanoparticles chemically modified with a fullerene derivative. *Sol. Energy Mater. Sol. Cells* **2007**, *91*, 1243–1247.
- (243) Lim, M. K.; Jang, S. R.; Vittal, R.; Lee, H.; Kim, K. J. Linking of N₃ dye with C-60 through diaminohydrocarbons for enhanced performance of dye-sensitized TiO₂ solar cells. *J. Photochem. Photobiol., A* **2007**, *190*, 128–134.
- (244) Gust, D.; Moore, T. A.; Moore, A. L. Photochemistry of supramolecular systems containing C-60. *J. Photochem. Photobiol., B* **2000**, *58*, 63–71.
- (245) Kamat, P. V.; Haria, M.; Hotchandani, S. C-60 cluster as an electron shuttle in a Ru(II)-polypyridyl sensitizer-based photochemical solar cell. *J. Phys. Chem. B* **2004**, *108*, 5166–5170.
- (246) D'Souza, F.; Chitta, R.; Sandanayaka, A. S. D.; Subbaiyan, N. K.; D'Souza, L.; Araki, Y.; Ito, O. Supramolecular carbon nanotube-fullerene donor-acceptor hybrids for photoinduced electron transfer. *J. Am. Chem. Soc.* **2007**, *129*, 15865–15871.
- (247) Kamat, P. V. Harvesting photons with carbon nanotubes. *Nano Today* **2006**, *1*, 20–27.
- (248) Cui, J.; Wang, A.; Edleman, N. L.; Ni, J.; Lee, P.; Armstrong, N. R.; Marks, T. J. Indium tin oxide alternatives - High work function transparent conducting oxides as anodes for organic light-emitting diodes. *Adv. Mater.* **2001**, *13*, 1476–1480.
- (249) van de Lagemaat, J.; Barnes, T. M.; Rumbles, G.; Shaheen, S. E.; Coutts, T. J.; Weeks, C.; Levitsky, I.; Peltola, J.; Glatkowski, P. Organic solar cells with carbon nanotubes replacing In₂O₃: Sn as the transparent electrode. *Appl. Phys. Lett.* **2006**, *88*, 233503.
- (250) Hu, L.; Hecht, D. S.; Gruner, G. Percolation in transparent and conducting carbon nanotube networks. *Nano Letters* **2004**, *4*, 2513–2517.
- (251) Wu, Z.; Chen, Z.; Du, X.; Logan, J. M.; Sippel, J.; Nikolou, M.; Kamaras, K.; Reynolds, J. R.; Tanner, D. B.; Hebard, A. F.; Rinzler, A. G. Transparent, conductive carbon nanotube films. *Science* **2004**, *305*, 1273–1276.
- (252) Aurelien Du, P.; Husnu Emrah, U.; Alokik, K.; Steve, M.; Manish, C. Conducting and transparent single-wall carbon nanotube electrodes for polymer-fullerene solar cells. *Appl. Phys. Lett.* **2005**, *87*, 203511.
- (253) Rowell, M. W.; Topinka, M. A.; McGehee, M. D.; Prall, H. J.; Dennler, G.; Saricifti, N. S.; Hu, L. B.; Gruner, G. Organic solar cells with carbon nanotube network electrodes. *Appl. Phys. Lett.* **2006**, *88*, 233506.
- (254) Mills, A.; LeHunte, S. An overview of semiconductor photo-catalysis. *J. Photochem. Photobiology., A* **1997**, *108*, 1–35.
- (255) Matsumoto, Y.; Unal, U.; Tanaka, N.; Kudo, A.; Kato, H. Electrochemical approach to evaluate the mechanism of photocatalytic water splitting on oxide photocatalysts. *J. Solid State Chem.* **2004**, *177*, 4205–4212.
- (256) Sheeney-Haj-Khia, L.; Basnar, B.; Willner, I. Efficient generation of photocurrents by using CdS/Carbon nanotube assemblies on electrodes. *Angew. Chem., Int. Ed.* **2005**, *44*, 78–83.
- (257) Haremza, J. M.; Hahn, M. A.; Krauss, T. D. Attachment of single CdSe nanocrystals to individual single-walled carbon nanotubes. *Nano Letters* **2002**, *2*, 1253–1258.
- (258) Khoshnevisan, B.; Behpour, M.; Ghoreishi, S. M.; Hemmati, M. Absorptions of hydrogen in Ag-CNTs electrode. *Int. J. Hydrogen Energy* **2007**, *32*, 3860–3863.
- (259) Michel, M.; Taylor, A.; Sekol, R.; Podsiadlo, P.; Ho, P.; Kotov, N.; Thompson, L. High-performance nanostructured membrane electrode, assemblies for fuel cells made by layer-by-layer assembly of carbon nanocolloids. *Adv. Mater.* **2007**, *19*, 3859–3864.
- (260) Britto, P. J.; Santhanam, K. S. V.; Rubio, A.; Alonso, J. A.; Ajayan, P. M. Improved charge transfer at carbon nanotube electrodes. *Adv. Mater.* **1999**, *11*, 154–157.
- (261) Wang, C.; Waje, M.; Wang, X.; Tang, J. M.; Haddon, R. C.; Yan, Y. S. Proton exchange membrane fuel cells with carbon nanotube based electrodes. *Nano Letters* **2004**, *4*, 345–348.
- (262) Li, W. Z.; Liang, C. H.; Zhou, W. J.; Qiu, J. S.; Zhou, Z. H.; Sun, G. Q.; Xin, Q. Preparation and characterization of multiwalled carbon nanotube-supported platinum for cathode catalysts of direct methanol fuel cells. *J. Phys. Chem. B* **2003**, *107*, 6292–6299.
- (263) Liu, Z. L.; Lin, X. H.; Lee, J. Y.; Zhang, W.; Han, M.; Gan, L. M. Preparation and characterization of platinum-based electrocatalysts on multiwalled carbon nanotubes for proton exchange membrane fuel cells. *Langmuir* **2002**, *18*, 4054–4060.
- (264) Ye, Y.; Ahn, C. C.; Witham, C.; Fultz, B.; Liu, J.; Rinzler, A. G.; Colbert, D.; Smith, K. A.; Smalley, R. E. Hydrogen adsorption and cohesive energy of single-walled carbon nanotubes. *Appl. Phys. Lett.* **1999**, *74*, 2307–2309.
- (265) Cheng, H. M.; Yang, Q. H.; Liu, C. Hydrogen storage in carbon nanotubes. *Carbon* **2001**, *39*, 1447–1454.
- (266) Kowalczyk, P.; Holyst, R.; Terrones, M.; Terrones, H. Hydrogen storage in nanoporous carbon materials: myth and facts. *Phys. Chem. Chem. Phys.* **2007**, *9*, 1786–1792.
- (267) Lee, S. M.; Lee, Y. H. Hydrogen storage in single-walled carbon nanotubes. *Appl. Phys. Lett.* **2000**, *76*, 2877–2879.
- (268) Dillon, A. C.; Heben, M. J. Hydrogen storage using carbon adsorbents: past, present and future. *Appl. Phys. A: Mater. Sci. Process.* **2001**, *72*, 133–142.
- (269) Schlapbach, L.; Züttel, A. Hydrogen-storage materials for mobile applications. *Nature* **2001**, *414*, 353–358.
- (270) Multi-Year Research, Development, And Demonstration Plan: Planned Program Activities for 2003–2010; U.S. Department of Energy: Washington, DC, 2007.
- (271) Lueking, A.; Yang, R. T. Hydrogen spillover from a metal oxide catalyst onto carbon nanotubes - Implications for hydrogen storage. *J. Catal.* **2002**, *206*, 165–168.
- (272) Benard, P.; Chahine, R.; Chandonia, P. A.; Cossement, D.; Dorval-Douville, G.; Lafi, L.; Lachance, P.; Paggiaro, R.; Poirier, E. Comparison of hydrogen adsorption on nanoporous materials. *J. Alloys Compd.* **2007**, *446*, 380–384.
- (273) Li, Y. W.; Yang, R. T. Hydrogen storage in metal-organic frameworks by bridged hydrogen spillover. *J. Am. Chem. Soc.* **2006**, *128*, 8136–8137.
- (274) Reddy, A. L. M.; Ramaprabhu, S. Hydrogen storage properties of nanocrystalline Pt dispersed multi-walled carbon nanotubes. *Int. J. Hydrogen Energy* **2007**, *32*, 3998–4004.
- (275) Zhang, D. J.; Ma, C.; Liu, C. B. Potential high-capacity hydrogen storage medium: Hydrogenated silicon fullerenes. *J. Phys. Chem. C* **2007**, *111*, 17099–17103.
- (276) Li, Y. W.; Yang, R. T. Significantly enhanced hydrogen storage in metal-organic frameworks via spillover. *J. Am. Chem. Soc.* **2006**, *128*, 726–727.
- (277) Li, G. Y.; Wang, P. M.; Zhao, X. Pressure-sensitive properties and microstructure of carbon nanotube reinforced cement composites. *Cem. Concr. Compos.* **2007**, *29*, 377–382.

- (278) Ajayan, P. M.; Zhou, O. Z. *In Carbon Nanotubes* **2001**, *80*, 391.
- (279) McKenzie, L. C.; Hutchison, J. E. Green nanoscience. *Chim. Oggi* **2004**, *22*, 30–33.
- (280) Eckelman, M.; Zimmerman, J.; Anastas, P., Toward green nano: Atom economy and *E*-factor analysis of several nanomaterial syntheses. *J. Ind. Ecol.*, in press.
- (281) Steinfeldt, M.; Gleich, A. v.; Petschow, U.; Haum, R. , *Nanotechnologies, Hazards and Resource Efficiency: A Three-Tiered Approach to Assessing the Implications of Nanotechnology and Influencing its Development*; Springer: Berlin, 2007.
- (282) Guldi, D. M.; Rahman, G. M. A.; Prato, M.; Jux, N.; Qin, S. H.; Ford, W. Single-wall carbon nanotubes as integrative building blocks for solar-energy conversion. *Angew. Chem., Int. Ed.* **2005**, *44*, 2015–2018.
- (283) Fischhoff, B.; Bostrom, A.; Quadrel, M., *In Oxford Textbook of Public Health*, 4th ed.; Detels, R., McEwen, J., Reaglehole, R., Tanaka, H., Eds; Oxford University Press: Oxford, UK, 2002.

ES8006904